

ELECTRONIC SUPPLEMENTARY INFORMATION (ESI) for

Glycosylated Metal Chelators as Anti-Parasitic Agents with Tunable Selectivity

Andrew Reddy[†], Leandro Stefano Sangenito[‡], Arthur de Azevedo Guedes[‡], Marta Helena Branquinho[‡], Kevin Kavanagh[§], John McGinley[~], André Luis Souza dos Santos^{‡*} and Trinidad Velasco-Torrijos^{†*}

[†] Department of Chemistry, Maynooth University, Maynooth, Co. Kildare, Ireland

[‡] Department of General Microbiology, Microbiology Institute Paulo de Góes, Federal University of Rio de Janeiro (UFRJ), Rio de Janeiro, RJ, 21941-590, Brazil

[§] Department of Biology, Maynooth University, Maynooth, Co. Kildare, Ireland

[~] Department of Chemistry, University of Copenhagen, DK-2100, Copenhagen, Denmark

Table of Contents

1. Crystallography

1.1 X-Ray crystallographic data for <i>cis</i> -aquadichloro(<i>N</i> -[4-(hydroxyphenyl)methyl]-2-pyridinemethamine)copper 3a .	3
1.2 X-Ray crystallographic data for 4-[(2-methylpyridinyl)- <i>E</i> -imino]methyl}-benzene-1,3-diol 6a .	6
1.3 X-Ray crystallographic data for 5-(2-hydroxyethoxy)-2-[(2-methylpyridinyl)- <i>E</i> -imino]methyl}phenol 6c .	8
1.4 X-Ray crystallographic data for bis(2-picolylamine)zinc perchlorate 9 .	10

2. Stability of the N₂ complexes

2.1 UV/Vis spectra of Cu(II) complex 3a in DMSO/water at 0 h, 24 h and 72 h.	13
2.2 ¹ H NMR spectra of Zn(II) complex 4 in d ₆ -DMSO/D ₂ O at 0 h and 72 h.	13

3. Biological Evaluation

3.1 Evaluation of <i>in vitro</i> cytotoxicity to macrophage cells	14
3.2 Evaluation of <i>in vivo</i> cytotoxicity to <i>Galleria mellonella</i> larvae	14

4. Synthetic procedures

4.1 General methods	15
4.2 Synthesis of 4-(2,3,4,6-tetra- <i>O</i> -acetyl-β- <i>D</i> -glucopyranosyloxy)benzaldehyde 1b	15
4.3 Synthesis of <i>N</i> -[4-(hydroxyphenyl)methyl]-2-pyridinemethamine 2a .	16
4.4 Synthesis of 2-hydroxy-4-(2,3,4,6-tetra- <i>O</i> -acetyl-β- <i>D</i> -glucopyranosyloxy)benzaldehyde 5b .	17
4.5 Synthesis of 2-hydroxy-4-(2-hydroxyethoxy)benzaldehyde 5c .	17
4.6 Synthesis of bis(2-picolylamine)zinc perchlorate 9 .	18

5. Spectroscopic data

5.1 ¹ H NMR spectrum of 4-(2,3,4,6-tetra-O-acetyl-β-D glucopyranosyloxy)benzaldehyde 1b .	19
5.2 ¹³ C NMR spectrum of 4-(2,3,4,6-tetra-O-acetyl-β-D-glucopyranosyloxy)benzaldehyde 1b .	19
5.3 ¹ H NMR spectrum of N-[4-(hydroxyphenyl)methyl]-2-pyridinemethamine 2a .	20
5.4 ¹³ C NMR spectrum of N-[4-(hydroxyphenyl)methyl]-2-pyridinemethamine 2a .	20
5.5 ¹ H NMR spectrum of N-{[4-(2,3,4,6-tetra-O-acetyl-β-D-glucopyranosyloxy)phenyl]methyl}-2-pyridinemethamine 2b .	21
5.6 ¹³ C NMR spectrum of N-{[4-(2,3,4,6-tetra-O-acetyl-β-D-glucopyranosyloxy)phenyl]methyl}-2-pyridinemethamine 2b .	21
5.7 FTIR spectrum of cis-aquadichloro(N-[4-(hydroxyphenyl)methyl]-2-pyridinemethamine)copper 3a .	22
5.8 FTIR spectrum of cis-dichloro(N-{[4-(2,3,4,6-tetra-O-acetyl-β-D-glucopyranosyloxy)phenyl]methyl}-2-pyridinemethamine)copper 3b .	23
5.9 ¹ H NMR spectrum of bis(N-[4-(hydroxyphenyl)methyl]-2-pyridinemethamine)zinc perchlorate monohydrate 4 .	23
5.10 ¹³ C NMR spectrum bis(N-[4-(hydroxyphenyl)methyl]-2-pyridinemethamine)zinc perchlorate monohydrate 4 .	23
5.11 ¹ H NMR spectrum of 2-hydroxy-4-(2,3,4,6-tetra-O-acetyl-β-D-glucopyranosyloxy)benzaldehyde 5b .	24
5.12 ¹³ C NMR spectrum of 2-hydroxy-4-(2,3,4,6-tetra-O-acetyl-β-D-glucopyranosyloxy)benzaldehyde 5b .	24
5.13 ¹ H NMR spectrum of 2-hydroxy-4-(2-hydroxyethoxy)benzaldehyde 5c .	25
5.14 ¹³ C NMR spectrum of 2-hydroxy-4-(2-hydroxyethoxy)benzaldehyde 5c .	25
5.15 ¹ H NMR spectrum of 2-chloroethyl 2,3,4,6-tetra-O-acetyl-β-D-glucopyranoside (starting material for the synthesis of 5d).	26
5.16 ¹³ C NMR spectrum of 2-chloroethyl 2,3,4,6-tetra-O-acetyl-β-D-glucopyranoside (starting material for the synthesis of 5d).	26
5.17 ¹ H NMR spectrum of 2-hydroxy-4-[2-(2,3,4,6-tetra-O-acetyl-β-D-glucopyranosyloxy)ethoxy]benzaldehyde 5d .	27
5.18 ¹³ C NMR spectrum of 2-hydroxy-4-[2-(2,3,4,6-tetra-O-acetyl-β-D-glucopyranosyloxy)ethoxy]benzaldehyde 5d .	27
5.19 ¹ H NMR spectrum of 4-[(2-methylpyridinyl)-E-imino]methyl}-benzene-1,3-diol 6a .	28
5.20 ¹³ C NMR spectrum of 4-[(2-methylpyridinyl)-E-imino]methyl}-benzene-1,3-diol 6a .	28
5.21 ¹ H NMR spectrum of 5-(2,3,4,6-tetra-O-acetyl-β-D-glucopyranosyloxy)-2-[(2-methylpyridinyl)-E-imino]methylphenol 6b .	29
5.22 ¹³ C NMR spectrum of 5-(2,3,4,6-tetra-O-acetyl-β-D-glucopyranosyloxy)-2-[(2-methylpyridinyl)-E-imino]methylphenol 6b .	29
5.23 ¹ H NMR spectrum of 5-(2-hydroxyethoxy)-2-[(2-methylpyridinyl)-E-imino]methyl}phenol 6c .	30
5.24 ¹³ C NMR spectrum of 5-(2-hydroxyethoxy)-2-[(2-methylpyridinyl)-E-imino]methyl}phenol 6c .	30

5.25 ¹ H NMR spectrum of 5-[2-(2,3,4,6-tetra-O-acetyl-β-D-glucopyranosyloxy)ethoxy)-2-[(2-methylpyridinyl)-E-imino]methyl]phenol 6d .	31
5.26 ¹³ C NMR spectrum of 5-[2-(2,3,4,6-tetra-O-acetyl-β-D-glucopyranosyloxy)ethoxy)-2-[(2-methylpyridinyl)-E-imino]methyl]phenol 6d .	31
5.27 FTIR spectrum of aqua(5-hydroxy-2-[(2-methylpyridinyl)-E-imino]methyl}phenoate)copper perchlorate dihydrate 7 .	32
5.28 ¹ H NMR spectrum of aqua(5-hydroxy-2-[(2-methylpyridinyl)-E-imino]methyl}phenoate)zinc perchlorate 8 .	33
5.29 ¹ H NMR spectrum bis(2-picolylamine)zinc perchlorate 9 .	33
5.30 ¹³ C NMR spectrum bis(2-picolylamine)zinc perchlorate 9 .	33

1. Crystallography

1.1 X-Ray crystallographic data for *cis-aquadichloro(N-[4-(hydroxyphenyl)methyl]-2-pyridinemethamine)copper 3a*.

Crystals suitable for X-ray crystal analysis were grown by dissolving the sample in warm (approx. 40 °C) MeCN and allowing the solution to cool slowly to room temperature and stand for several days in the dark to yield small green crystals. This was found to display a triclinic structure with a two different copper species present in the unit cell. At the vertices of the cell there are dimers of a 1:1 pentacoordinate copper complex which displays a distorted square-pyramidal coordination geometry with one terminal chloride and two bridging chloride ligands. Encapsulated in the unit cell are two molecules of a mononuclear pentacoordinate square pyramidal copper complex exhibiting two terminal chloride ligands and an acetonitrile molecule occupying the axial position. Elemental analysis indicates that the bulk material synthesized contains a water molecule and it is likely that this occupies the axial position in place of the acetonitrile observed in the crystal structure.

A specimen of **3a**, approximate dimensions 0.120 mm x 0.180 mm x 0.230 mm, was used for the X-ray crystallographic analysis. The X-ray intensity data were measured at 100(2)K using an Oxford Cryosystems Cobra low temperature device using a MiTeGen micromount. Bruker APEX software was used to correct for Lorentz and polarization effects.

A total of 901 frames were collected. The total exposure time was 2.50 hours. The integration of the data using a triclinic unit cell yielded a total of 58825 reflections to a maximum θ angle of 30.21° (0.71 Å resolution), of which 8816 were independent (average redundancy 6.673, completeness = 99.4%, Rint = 2.82%, Rsig = 1.86%) and 7707 (87.42%) were greater than 2 σ (F₂). The final cell constants of $a = 11.9914(6)$ Å, $b = 12.6755(6)$ Å, $c = 12.6960(6)$ Å, $\alpha = 113.9980(10)^\circ$, $\beta = 96.5800(10)^\circ$, $\gamma = 115.3470(10)^\circ$, volume = 1492.65(13) Å³, are based upon the refinement of the XYZ-centroids of reflections above 20 σ (I). Data were corrected for absorption effects using the Multi-Scan method (SADABS). The ratio of minimum to maximum apparent transmission was 0.925. The calculated minimum and maximum transmission coefficients (based on crystal size) are 0.6898 and 0.7460.

The structure was solved and refined using the Bruker SHELXTL Software Package, using the space group $P\bar{1}$, with $Z = 1$ for the formula unit, C₅₆H₆₂Cl₈Cu₄N₁₀O₄. The final anisotropic full-matrix least-squares refinement on F² with 381 variables converged at R1 = 2.23%, for the observed data

and $wR2 = 5.72\%$ for all data. The goodness-of-fit was 1.030. The largest peak in the final difference electron density synthesis was $0.423 \text{ e}/\text{\AA}^3$ and the largest hole was $-0.420 \text{ e}/\text{\AA}^3$ with an RMS deviation of $0.062 \text{ e}/\text{\AA}^3$. On the basis of the final model, the calculated density was $1.643 \text{ g}/\text{cm}^3$ and $F(000)$, 752 e $^-$.

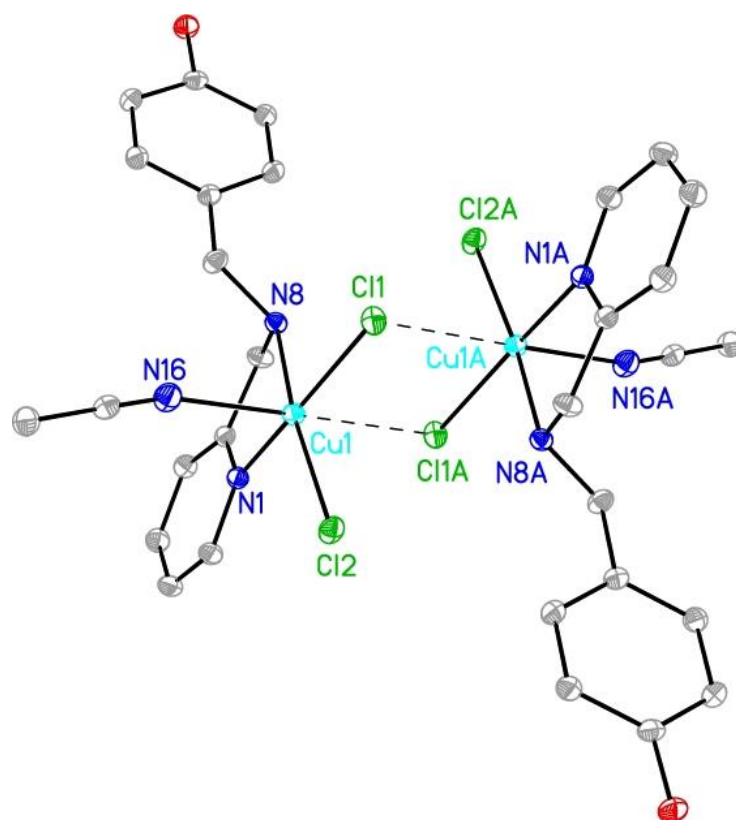


Figure 1.1-ESI: X-ray crystal structure of Cu(II) complex **3a** (acetonitrile adduct).

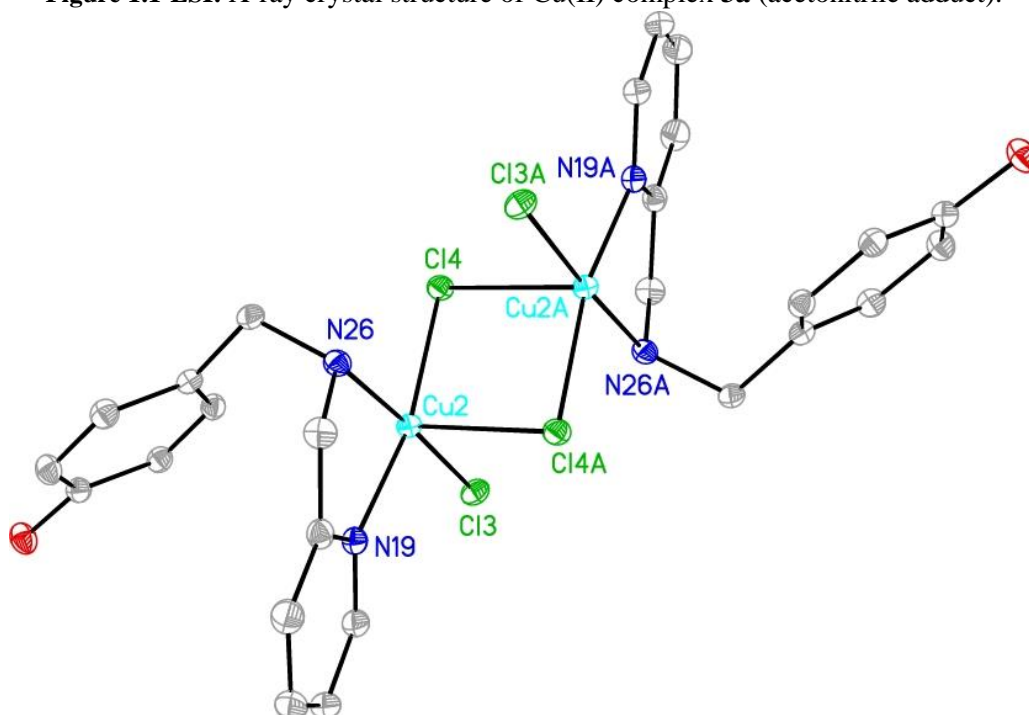


Figure 1.2-ESI: X-ray crystal structure of Cu(II) complex **3a** (chloride bridged dimer).

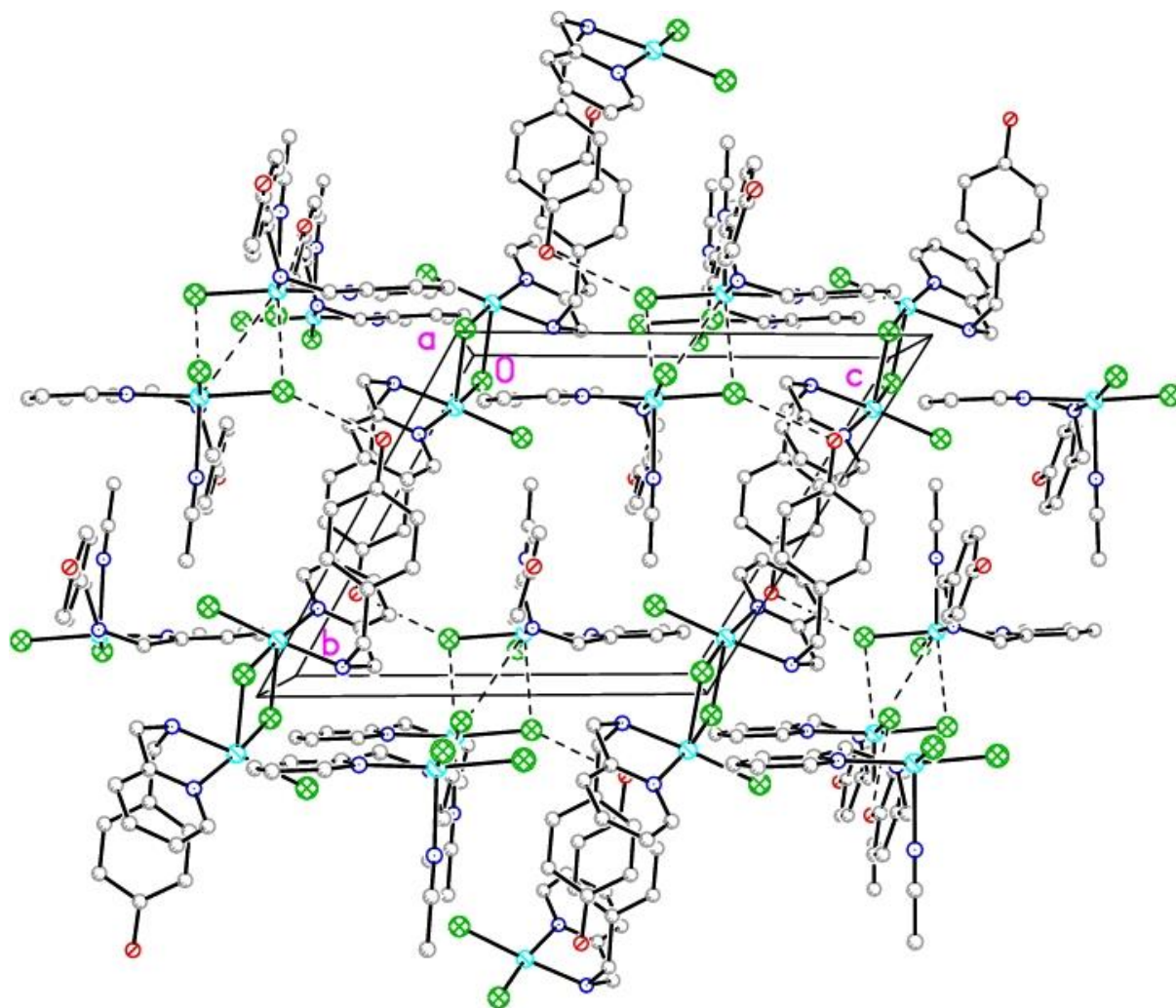


Figure 1.3-ESI: X-ray crystal structure of Cu(II) complex **3a** (unit cell).

Empirical formula	$C_{56}H_{62}C_{18}Cu_4N_{10}O_4$	
Formula weight	1476.91	
Temperature	100(2) K	
Wavelength	0.71073 Å	
Crystal system	Triclinic	
Space group	$P\bar{1}$	
Unit cell dimensions	$a = 11.9914(6)$ Å $b = 12.6755(6)$ Å $c = 12.6960(6)$ Å	$\alpha = 113.9980(10)^\circ$. $\beta = 96.5800(10)^\circ$. $\gamma = 115.3470(10)^\circ$.
Volume	$1492.64(13)$ Å ³	
Z	1	
Density (calculated)	1.643 Mg/m ³	
Absorption coefficient	1.819 mm ⁻¹	
F(000)	752	
Crystal size	0.230 x 0.180 x 0.120 mm ³	
Theta range for data collection	1.874 to 30.211°	
Index ranges	$-16 \leq h \leq 16$, $-17 \leq k \leq 17$, $-17 \leq l \leq 17$	
Reflections collected	58825	
Independent reflections	8816 [R(int) = 0.0282]	
Completeness to theta = 25.242°	100.0 %	
Absorption correction	Semi-empirical from equivalents	

Max. and min. transmission	0.7460 and 0.6898
Refinement method	Full-matrix least-squares on F ²
Data / restraints / parameters	8816 / 0 / 381
Goodness-of-fit on F ²	1.030
Final R indices [I > 2σ(I)]	R1 = 0.0223, wR2 = 0.0542
R indices (all data)	R1 = 0.0292, wR2 = 0.0572
Largest diff. peak and hole	0.423 and -0.420 e.Å ⁻³

1.2 X-Ray crystallographic data for -{[(2-methylpyridinyl)-E-imino]methyl}-benzene-1,3-diol **6a**.

Crystals suitable for x-ray crystallography were grown by dissolving the sample in hot acetonitrile and letting the sample stand for several hours to yield pale orange trapezoid-like crystals.

A clear light yellow trapezoid-like specimen of C₁₃H₁₂N₂O₂, approximate dimensions 0.200 mm x 0.200 mm x 0.280 mm, was used for the X-ray crystallographic analysis. The X-ray intensity data were measured at 100(2)K using an Oxford Cryosystems low temperature device using a MiTeGen micromount. See Table 1 for collection parameters and exposure time. Bruker APEX software was used to correct for Lorentz and polarization effects.

A total of 630 frames were collected. The total exposure time was 1.25 hours. The frames were integrated with the Bruker SAINT software package using a narrow-frame algorithm. The integration of the data using a monoclinic unit cell yielded a total of 8049 reflections to a maximum θ angle of 28.26° (0.75 Å resolution), of which 2810 were independent (average redundancy 2.864, completeness = 99.6%, Rint = 2.58%, Rsig = 2.91%) and 2250 (80.07%) were greater than 2σ(F₂). The final cell constants of a = 22.8835(13) Å, b = 5.7669(3) Å, c = 18.6703(10) Å, β = 112.5980(15)°, volume = 2274.7(2) Å³, are based upon the refinement of the XYZ-centroids of 6350 reflections above 20 σ(I) with 7.159° < 2θ < 56.46°. Data were corrected for absorption effects using the Multi-Scan method (SADABS). The ratio of minimum to maximum apparent transmission was 0.949. The calculated minimum and maximum transmission coefficients (based on crystal size) are 0.7075 and 0.7457.

The structure was solved and refined using the Bruker SHELXTL Software Package, using the space group C2/c, with Z = 8 for the formula unit, C₁₃H₁₂N₂O₂. The final anisotropic full-matrix least-squares refinement on F² with 163 variables converged at R1 = 3.91%, for the observed data and wR2 = 10.34% for all data. The goodness-of-fit was 1.026. The largest peak in the final difference electron density synthesis was 0.359 e-/Å³ and the largest hole was -0.213 e-/Å³ with an RMS deviation of 0.044 e-/Å³. On the basis of the final model, the calculated density was 1.333 g/cm³ and F(000), 960 e-.

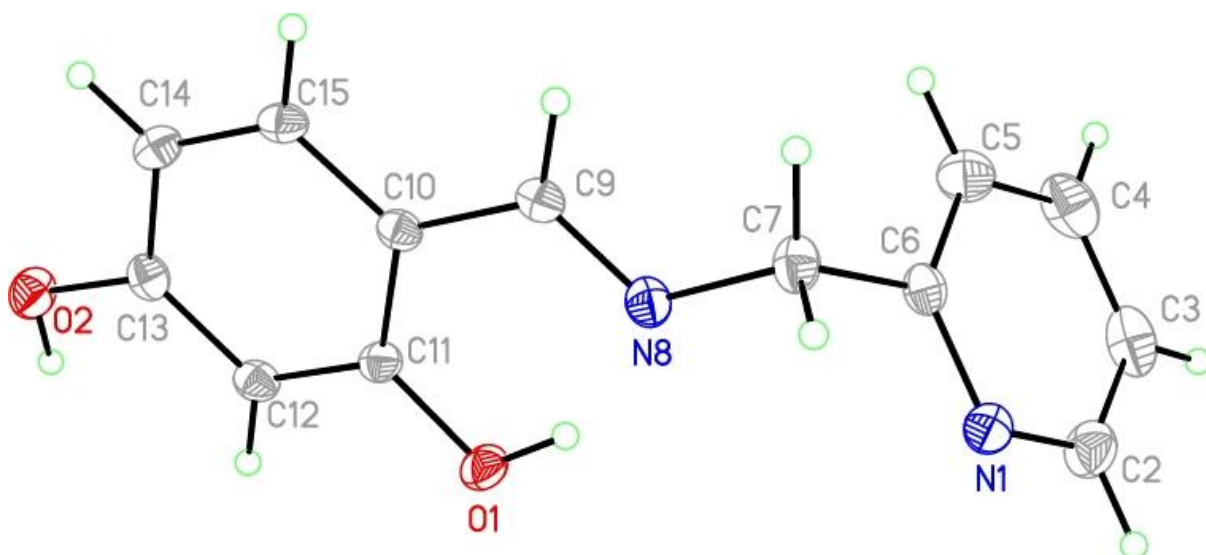


Figure 1.4-ESI: X-ray crystal structure of ligand **6a**.

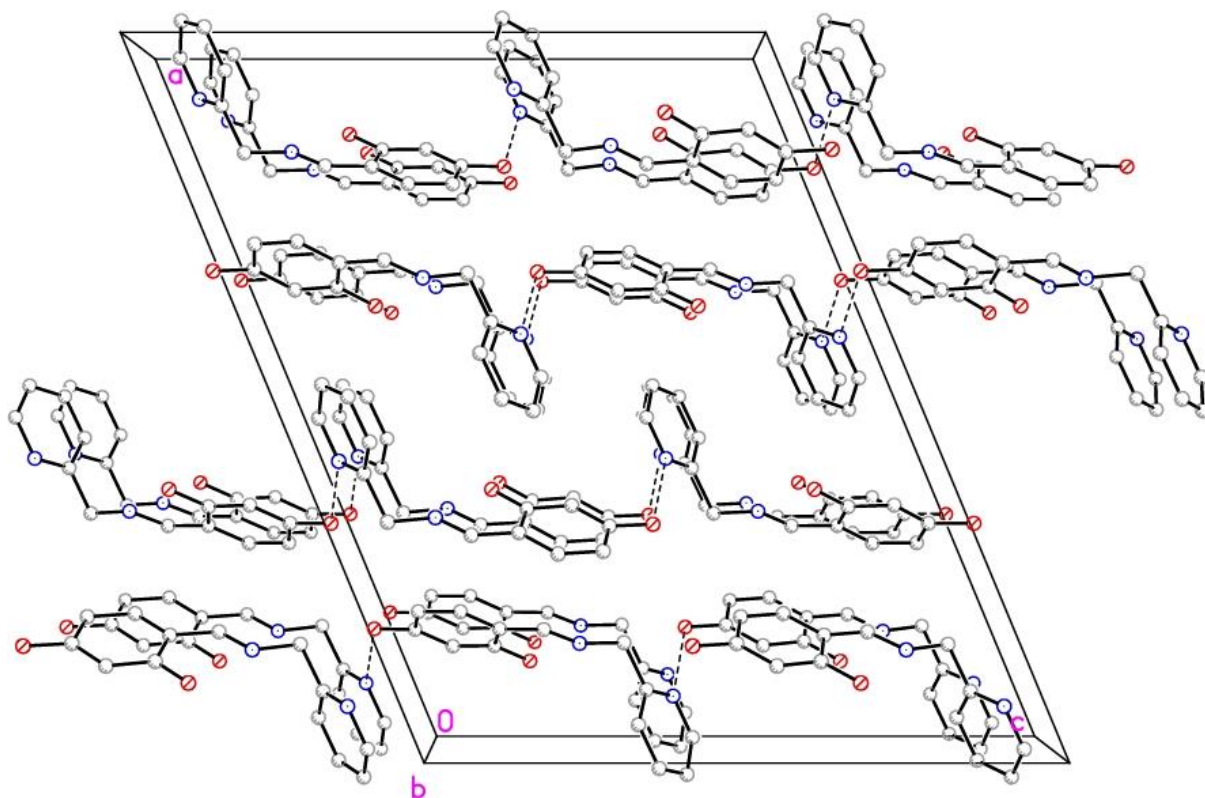


Figure 1.5-ESI: X-ray crystal structure of ligand **6a** (unit cell).

Empirical formula	$C_{13}H_{12}N_2O_2$
Formula weight	228.25
Temperature	99.92 K
Wavelength	0.71073 Å
Crystal system	Monoclinic
Space group	C2/c

Unit cell dimensions	a = 22.8835(13) Å b = 5.7669(3) Å c = 18.6703(10) Å	$\alpha = 90^\circ$. $\beta = 112.5980(15)^\circ$. $\gamma = 90^\circ$.
Volume	2274.7(2) Å ³	
Z	8	
Density (calculated)	1.333 Mg/m ³	
Absorption coefficient	0.092 mm ⁻¹	
F(000)	960	
Crystal size	0.28 x 0.2 x 0.2 mm ³	
Theta range for data collection	3.580 to 28.260°.	
Index ranges	-30 ≤ h ≤ 28, -7 ≤ k ≤ 5, -18 ≤ l ≤ 24	
Reflections collected	8049	
Independent reflections	2810 [R(int) = 0.0258]	
Completeness to theta = 25.242°	99.6 %	
Absorption correction	Semi-empirical from equivalents	
Max. and min. transmission	0.7457 and 0.7075	
Refinement method	Full-matrix least-squares on F ²	
Data / restraints / parameters	2810 / 0 / 163	
Goodness-of-fit on F ²	1.026	
Final R indices [I > 2σ(I)]	R1 = 0.0391, wR2 = 0.0949	
R indices (all data)	R1 = 0.0529, wR2 = 0.1034	
Extinction coefficient	0.0049(6)	
Largest diff. peak and hole	0.359 and -0.213 e.Å ⁻³	

1.3 X-Ray crystallographic data for 5-(2-hydroxyethoxy)-2-[(2-methylpyridinyl)-E-imino]methylphenol **6c**.

Crystals suitable for x-ray crystallography were grown by dissolving the sample in hot acetonitrile and allowing it to cool for several hours which yielded long needle shaped crystals.

A specimen of C₁₅H₁₆N₂O₃, approximate dimensions 0.120 mm x 0.170 mm x 0.350 mm, was used for the X-ray crystallographic analysis. The X-ray intensity data were measured at 100(2)K using an Oxford Cryosystems low temperature device using a MiTeGen micromount. See Table 1 for collection parameters and exposure time. Bruker APEX software was used to correct for Lorentz and polarization effects.

A total of 1246 frames were collected. The total exposure time was 3.60 hours. The frames were integrated with the Bruker SAINT software package using a narrow-frame algorithm. The integration of the data using a monoclinic unit cell yielded a total of 32488 reflections to a maximum θ angle of 33.14° (0.65 Å resolution), of which 5038 were independent (average redundancy 6.449, completeness = 99.7%, Rint = 4.95%, Rsig = 3.82%) and 3656 (72.57%) were greater than 2σ(F²). The final cell constants of a = 5.3704(2) Å, b = 20.0520(5) Å, c = 12.4990(4) Å, β = 100.5131(15)°, volume = 1323.39(7) Å³, are based upon the refinement of the XYZ-centroids of 9944 reflections above 20 σ(I) with 5.243° < 2θ < 66.20°. Data were corrected for absorption effects using the Multi-Scan method (SADABS). The ratio of minimum to maximum apparent transmission was 0.918. The calculated minimum and maximum transmission coefficients (based on crystal size) are 0.6856 and 0.7465.

The structure was solved and refined using the Bruker SHELXTL Software Package, using the space group P21/c, with $Z = 4$ for the formula unit, $C_{15}H_{16}N_2O_3$. The final anisotropic full-matrix least-squares refinement on F^2 with 189 variables converged at $R1 = 4.87\%$, for the observed data and $wR2 = 12.71\%$ for all data. The goodness-of-fit was 1.037. The largest peak in the final difference electron density synthesis was $0.408 \text{ e}/\text{\AA}^3$ and the largest hole was $-0.272 \text{ e}/\text{\AA}^3$ with an RMS deviation of $0.062 \text{ e}/\text{\AA}^3$. On the basis of the final model, the calculated density was $1.367 \text{ g}/\text{cm}^3$ and $F(000)$, 576 e $^-$.

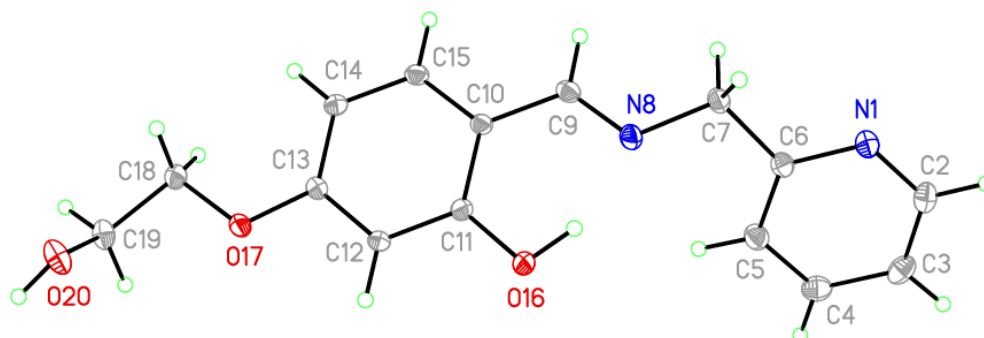


Figure 1.6-ESI: X-ray crystal structure of ligand **6c**.

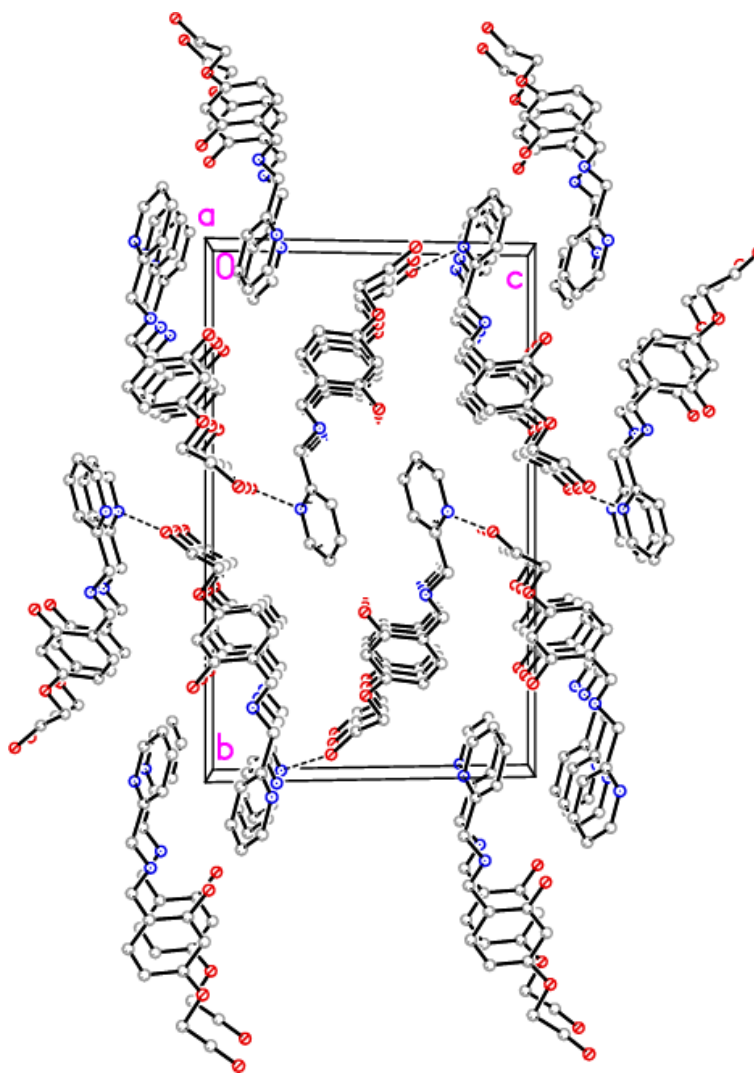


Figure 1.7-ESI: X-ray crystal structure of ligand **6c** (unit cell).

Empirical formula	C ₁₅ H ₁₆ N ₂ O ₃	
Formula weight	272.30	
Temperature	99.99 K	
Wavelength	0.71073 Å	
Crystal system	Monoclinic	
Space group	P21/c	
Unit cell dimensions	a = 5.3704(2) Å b = 20.0520(5) Å c = 12.4990(4) Å	α = 90°. β = 100.5131(15)°. γ = 90°.
Volume	1323.39(7) Å ³	
Z	4	
Density (calculated)	1.367 Mg/m ³	
Absorption coefficient	0.096 mm ⁻¹	
F(000)	576	
Crystal size	0.35 x 0.17 x 0.12 mm ³	
Theta range for data collection	2.622 to 33.144°.	
Index ranges	-8 ≤ h ≤ 8, -30 ≤ k ≤ 30, -17 ≤ l ≤ 19	
Reflections collected	32488	
Independent reflections	5038 [R(int) = 0.0495]	
Completeness to theta = 26.000°	99.9 %	
Absorption correction	Semi-empirical from equivalents	
Max. and min. transmission	0.7465 and 0.6856	
Refinement method	Full-matrix least-squares on F ²	
Data / restraints / parameters	5038 / 0 / 189	
Goodness-of-fit on F ²	1.037	
Final R indices [I > 2σ(I)]	R1 = 0.0487, wR2 = 0.1130	
R indices (all data)	R1 = 0.0774, wR2 = 0.1271	
Largest diff. peak and hole	0.408 and -0.272 e.Å ⁻³	

1.4 X-Ray crystallographic data for bis(2-picolylamine)zinc perchlorate **9**.

Gray, rhombic like crystals suitable for X-ray analysis were obtained from the NMR sample of **8** prepared in d⁸-THF.

A specimen of C₁₂H₁₆Cl₂N₄O₈Zn, approximate dimensions 0.100 mm x 0.120 mm x 0.180 mm, was used for the X-ray crystallographic analysis. The X-ray intensity data were measured at 100(2)K using an Oxford Cryosystems low temperature device using a MiTeGen micromount. See Table 1 for collection parameters and exposure time. Bruker APEX software was used to correct for Lorentz and polarization effects.

A total of 472 frames were collected. The total exposure time was 0.92 hours. The frames were integrated with the Bruker SAINT software package using a wide-frame algorithm. The integration of the data using a tetragonal unit cell yielded a total of 21050 reflections to a maximum θ angle of 28.29° (0.75 Å resolution), of which 2120 were independent (average redundancy 9.929, completeness = 100.0%, R_{int} = 4.36%, R_{sig} = 2.35%) and 1832 (86.42%) were greater than 2σ(F²). The final cell constants of a = 14.9255(7) Å, b = 14.9255(7) Å, c = 15.3140(7) Å, volume = 3411.5(4) Å³, are based upon the refinement of the XYZ-centroids of

5191 reflections above 2θ $\sigma(I)$ with $5.458^\circ < 2\theta < 55.32^\circ$. Data were corrected for absorption effects using the Multi-Scan method (SADABS). The ratio of minimum to maximum apparent transmission was 0.900. The calculated minimum and maximum transmission coefficients (based on crystal size) are 0.6711 and 0.7457.

The structure was solved using the Bruker APEX Software Package and refined with Olex2, using the space group $I4_1/a$, with $Z = 8$ for the formula unit, $C_{12}H_{16}Cl_2N_4O_8Zn$. The final anisotropic full-matrix least-squares refinement on F^2 with 160 variables converged at $R1 = 5.00\%$, for the observed data and $wR2 = 10.18\%$ for all data. The goodness-of-fit was 1.280. The largest peak in the final difference electron density synthesis was $0.381 \text{ e}^-/\text{\AA}^3$ and the largest hole was $-0.528 \text{ e}^-/\text{\AA}^3$ with an RMS deviation of $0.091 \text{ e}^-/\text{\AA}^3$. On the basis of the final model, the calculated density was 1.871 g/cm^3 and $F(000)$, 1952 e^- .

Refinement Note: Perchlorate oxygen atoms modelled in two positions with occupancies of 69/31%.

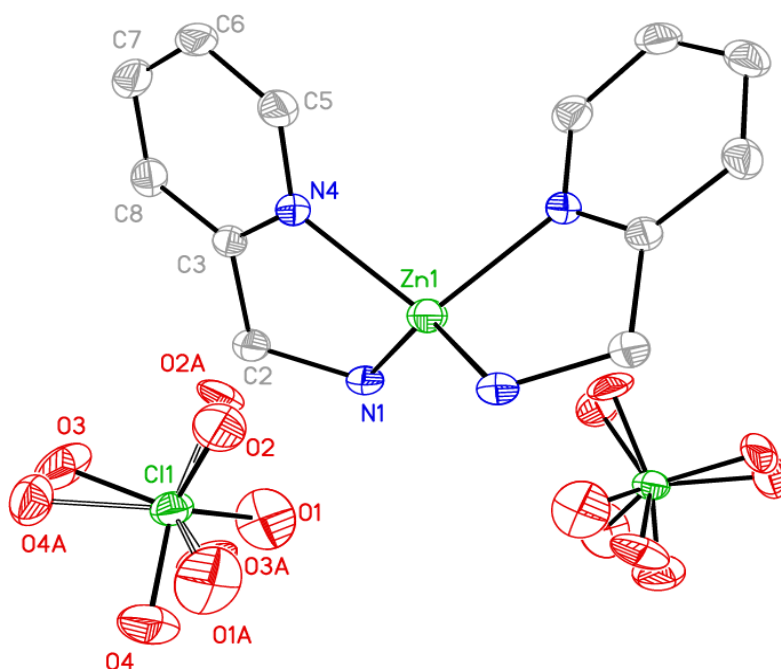


Figure 1.8-ESI: X-ray crystal structure of Zn(II) complex **9**.

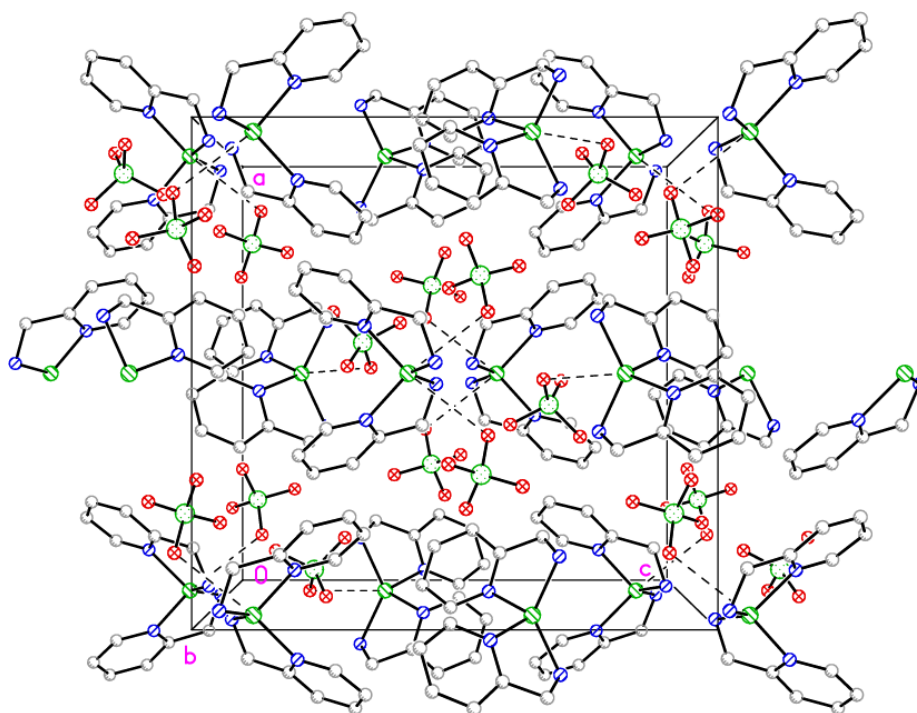


Figure 1.9-ESI: X-ray crystal structure of Zn(II) complex **9** (unit cell).

Empirical formula	$\text{C}_{12}\text{H}_{16}\text{Cl}_2\text{N}_4\text{O}_8\text{Zn}$	
Formula weight	480.56	
Temperature	99.99 K	
Wavelength	0.71073 Å	
Crystal system	Tetragonal	
Space group	$I4_1/a$	
Unit cell dimensions	$a = 14.9255(7)$ Å	$\alpha = 90^\circ$.
	$b = 14.9255(7)$ Å	$\beta = 90^\circ$.
	$c = 15.3140(7)$ Å	$\gamma = 90^\circ$.
Volume	$3411.5(4)$ Å ³	
Z	8	
Density (calculated)	1.871 Mg/m^3	
Absorption coefficient	1.806 mm^{-1}	
F(000)	1952	
Crystal size	$0.18 \times 0.12 \times 0.1 \text{ mm}^3$	
Theta range for data collection	1.905 to 28.289° .	
Index ranges	$-19 \leq h \leq 19$, $-17 \leq k \leq 19$, $-20 \leq l \leq 18$	
Reflections collected	21050	
Independent reflections	2120 [$R(\text{int}) = 0.0436$]	
Completeness to theta = 26.000°	100.0 %	

Absorption correction	Semi-empirical from equivalents
Max. and min. transmission	0.7457 and 0.6711
Refinement method	Full-matrix least-squares on F ²
Data / restraints / parameters	2120 / 0 / 160
Goodness-of-fit on F ²	1.280
Final R indices [I>2σ(I)]	R1 = 0.0500, wR2 = 0.0984
R indices (all data)	R1 = 0.0606, wR2 = 0.1018
Largest diff. peak and hole	0.381 and -0.528 e.Å ⁻³

2. Stability of the N₂ complexes

2.1 UV/Vis spectra of Cu(II) complex **3a** in DMSO/water a 0 h, 24 h and 72 h.

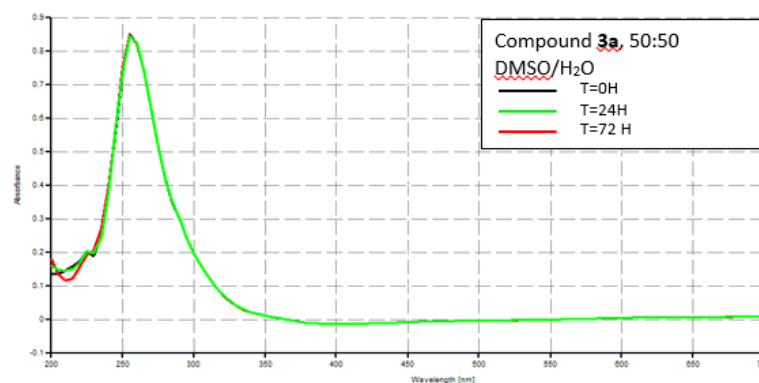


Figure 2.1-ESI: UV/Vis spectra of **3a** in DMSO/water a 0 h, 24 h and 72 h.

2.2 ¹H NMR spectra of Zn(II) complex **4** in d₆-DMSO/D₂O a 0 h and 72 h.

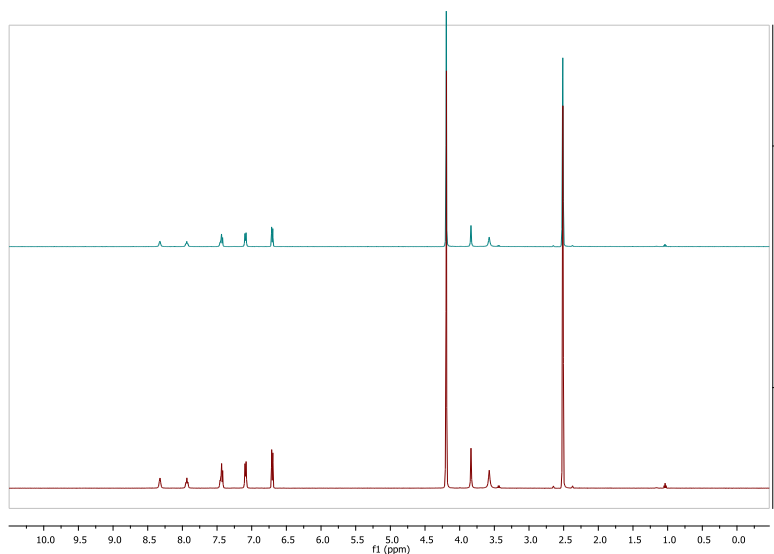


Figure 2.2-ESI: ¹H NMR spectra of **4** in d₆-DMSO/D₂O a 0 h (top) and 72 h (bottom).

3. Biological Evaluation

3.1 Evaluation of *in vitro* cytotoxicity to macrophage cells

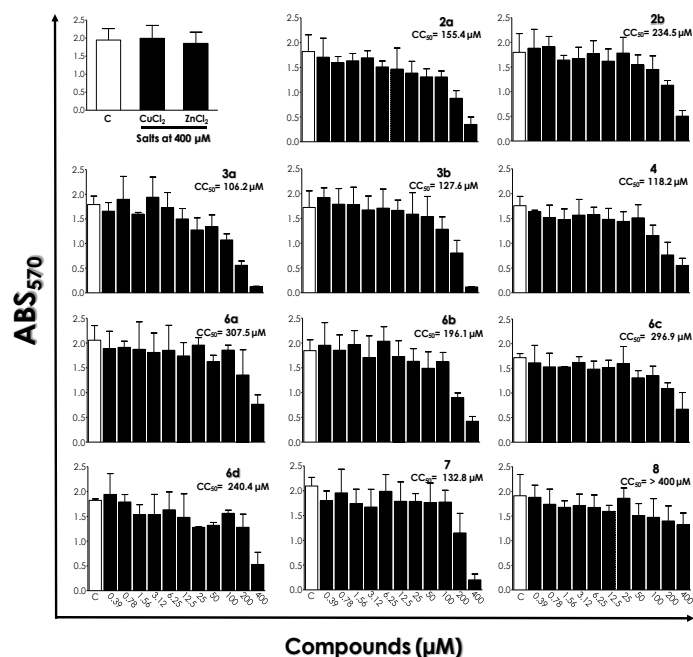


Figure 3.1-ESI. Cytotoxicity of amino/imino pyridyl derivatives on RAW macrophages. Initially, mammalian cells (105 cells) were incubated in a 96-well plate for 48 h (RAW) in the absence (white bars) or in the presence of single doses of the compounds at different concentrations (as indicated) (black bars). After that, the viability was determined spectrophotometrically at 570 nm (ABS, absorbance) by MTT assay. The CC₅₀ values are plotted for each compound. Data shown are the mean ± standard deviation (SD) of three independent experiments performed in triplicate.

3.2 Evaluation of *in vivo* cytotoxicity to *Galleria mellonella* larvae.

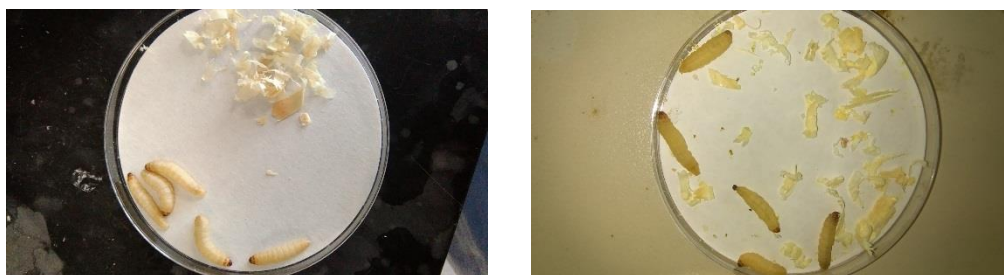


Figure 3.2-SI: *G. mellonella* larvae; left: immediately following inoculation of active compounds; right: 48 h after inoculation.

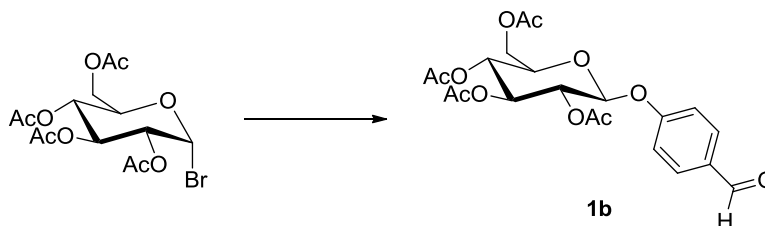
4. Synthetic procedures

4.1 General methods

All chemicals purchased were reagent grade and used without further purification unless stated otherwise. Dichloromethane and acetonitrile were freshly distilled over CaH₂ prior use. Ethanol was dried over 3 Å molecular sieves, which were flame dried prior to use. Reactions were monitored with thin layer chromatography (TLC) on Merck Silica Gel F₂₅₄ plates. Detection was effected by UV or charring in a mixture of 5% sulfuric acid-ethanol. All glassware used for anhydrous reactions was flame dried under vacuum prior to use. NMR spectra were obtained on a Bruker Ascend 500 or a Bruker Avance 300 spectrometer using the residual solvent peak as internal standard. Chemical shifts are reported in ppm. Flash chromatography was performed with Merck Silica Gel 60. Microwave reactions were carried out using a CEM Discover Microwave Synthesizer. Optical rotations were obtained from an AA-100 polarimeter. $[\alpha]_D$ values are given in 10⁻¹ cm²·g⁻¹. The melting points were obtained using a Stuart Scientific SMP1 melting point apparatus and are uncorrected. Purity was confirmed by elemental analysis using a FLASH EA 1112 Series Elemental Analyzer with Eager 300 operating software. High resolution mass spectrometry (HRMS) was performed on an Agilent-LC 1200 Series coupled to a 6210 Agilent Time-Of-Flight (TOF) mass spectrometer equipped with an electrospray source in both positive and negative (ESI+/-) modes. Magnetic susceptibility measurements were carried out at rt using a Johnson Matthey Magnetic Susceptibility Balance with [HgCo(SCN)₄] as reference. Infrared spectra were obtained as a film on NaCl plates or as KBr disks in the region 4000–400 cm⁻¹ on a Perkin Elmer Spectrum 100 FT-IR spectrophotometer. The detailed experimental procedures can be found in the Supporting Information.

Caution: Although not encountered in our experiments, perchlorate salts of metal ions are potentially explosive and should be manipulated with care.

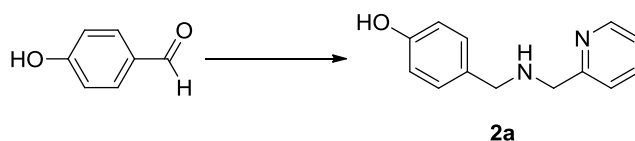
4.2 Synthesis of 4-(2,3,4,6-tetra-*O*-acetyl- β -D-glucopyranosyloxy)benzaldehyde **1b**



2, 3, 4, 6-Tetra-*O*-acetyl- α -D-glucopyranosyl bromide (5.68 g, 13.8 mmol), 4-hydroxybenzaldehyde (3.37 g, 17.6 mol) and silver (I) oxide (8 g, 34.5 mmol) were dissolved in freshly distilled anhydrous acetonitrile (80 mL) under nitrogen atmosphere. The reaction mixture was allowed to stir in the dark at rt for 17 h with approximately 1 g of 3 Å molecular sieves. The solvent was removed *in vacuo* and the residue was then dissolved in ethyl acetate and filtered through a Celite plug. The filtrate was then washed with 1 M HCl (100 mL), aq NaHCO₃ saturated solution (3 x 100 mL), brine (100 mL) and dried (Na₂SO₄). The mixture was filtered and the solvent was removed *in vacuo* to yield an orange solid which was recrystallized from ethanol: white solid (3.93 g, 63%).

Mp: 145-146°C. ^1H NMR (500 MHz, CDCl_3) δ 9.93 (s, 1H, C(=O)H), 7.85 (d, J = 8.7 Hz, 2H, Ar-H), 7.10 (d, J = 8.7 Hz, 2H, Ar-H), 5.41 – 5.26 (m, 2H, H-2, H-3), 5.27 – 4.88 (m, 2H, H-1, H-4), 4.29 (dd, J = 12.3, 5.5 Hz, 1H, H-6), 4.18 (dd, J = 12.3, 2.4 Hz, 1H, H-6'), 3.93 (ddd, J = 9.9, 5.5, 2.4 Hz, 1H, H-5), 2.07, 2.06, 2.06, 2.05 (each s, 3H, OAc). ^{13}C NMR (126 MHz, CDCl_3) δ 190.8 (HC=O), 170.6, 170.3, 169.5, 169.3 (each C=O), 161.3 (Ar-C), 131.9 (Ar-CH), 131.8 (Ar-C), 116.9 (Ar-CH), 98.2 (C-1), 72.7 (C-2), 72.5 (C-5), 71.2 (C-3), 68.3 (C-4), 62.1 (C-6), 20.8, 20.8, 20.7, 20.7 (each OAc). IR (KBr disk): 2963, 2850, 2747, 1754, 1692, 1505, 1422, 1380, 1233, 1038 cm^{-1} . HRMS (ESI+): m/z calculated for $\text{C}_{21}\text{H}_{24}\text{O}_{11} + \text{Na}^+$ $[\text{M} + \text{Na}^+]$: 475.1216. Found: 475.1201. $[\alpha]_{\text{D}}^{25}$: -0.17 (c 1, dichloromethane). NMR data is in agreement with that reported in the literature.ⁱ

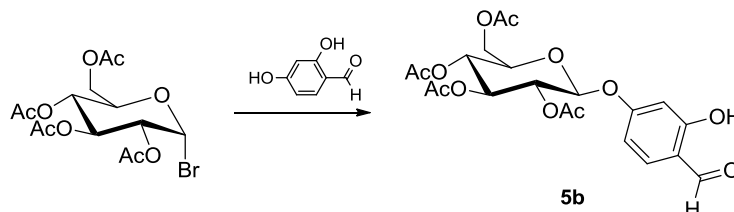
4.3 Synthesis of *N*-[4-(hydroxyphenyl)methyl]-2-pyridinemethamine **2a**



A mixture of 4-hydroxybenzaldehyde (10 g, 81.8 mmol), 2-aminomethylpyridine (8.76 mL, 85 mmol) and Na_2SO_4 (15 g, 0.1 mol) were refluxed in diethyl ether (200 mL) for 16 h. The solvent was removed on the rotatory evaporator to ~40 mL and the mixture was cooled to -10 °C in an ice/acetone/ NaCl bath. Ethanol (100 mL) was added. Sodium borohydride (9 g, 238 mmol) was added portion wise over 30 min. The reaction mixture was allowed to warm to rt and stir overnight. The reaction was quenched with water (~40 mL) and stirred until evolution of gas ceased. Ethanol was removed from the mixture on the rotatory evaporator and the remaining aqueous phase was extracted with diethyl ether (5 x 50 mL) and the combined organic extracts were washed with water (100 mL), brine (100 mL) and dried (Na_2SO_4). The mixture was filtered and the solvent was removed *in vacuo* to yield the product: brown syrup (12.41 g, 71%).

^1H NMR (500 MHz, CDCl_3) δ 8.52 (d, J = 5.4 Hz, 1H, Pyr-H), 7.64 (td, J = 7.7, 1.7 Hz, 1H, Pyr-H), 7.32 (d, J = 7.7 Hz, 1H, Pyr-H), 7.18 (dd, J = 7.0, 5.4 Hz, 1H, Pyr-H), 7.04 (d, J = 8.4 Hz, 2H, Ar-H), 6.62 (d, J = 8.4 Hz, 2H, Ar-H), 6.54 (s, 2H, N-H, O-H), 3.92 (s, 2H, CH_2), 3.72 (s, 2H, CH_2). ^{13}C NMR (126 MHz, CDCl_3) δ 158.8 (Pyr-C), 156.3 (Ar-C), 148.9 (Pyr-CH), 137.2 (Pyr-CH), 130.1 (Ar-C), 129.9 (Ar-CH), 129.8 (Ar-CH), 123.0 (Pyr-CH), 122.5 (Pyr-CH), 115.8 (Ar-CH), 115.5 (Ar-CH), 53.5 (Pyr- CH_2), 52.8 (Ar- CH_2). IR (film on NaCl): 3430, 3204, 3015, 2926, 1613, 1595, 1571, 1514, 1436, 1365, 1247, 1171, 831, 761, 565, 509 cm^{-1} . HRMS (ESI+): m/z calculated for $\text{C}_{13}\text{H}_{14}\text{N}_2\text{O} + \text{H}^+$ $[\text{M} + \text{H}^+]$: 215.1184. Found: 215.1187. Elemental analysis calculated (%) for $\text{C}_{13}\text{H}_{14}\text{N}_2\text{O}$: C 72.87, H 6.59, N 13.07. Found: C 72.76, H 6.88, N 12.96. NMR data is in agreement with that reported in the literature.ⁱⁱ

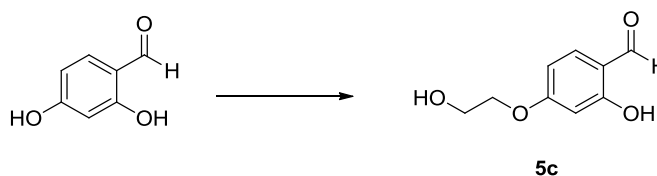
4.4 Synthesis of 2-hydroxy-4-(2,3,4,6-tetra-*O*-acetyl- β -D-glucopyranosyloxy)benzaldehyde **5b**.



2, 3, 4, 6-tetra-*O*-acetyl- α -D-glucopyranosyl bromide (2 g, 4.9 mmol), 2, 4-dihydroxybenzaldehyde (1.34 g, 9.7 mmol) and silver (I) carbonate (2.70 g, 9.7 mmol) were dissolved in freshly distilled acetonitrile (50 mL) under nitrogen atmosphere. The reaction mixture was stirred in the dark at rt for 17 h. The solvent was removed *in vacuo* and the residue was dissolved in ethyl acetate (80 mL) with sonication and filtered through a Celite cake. The filtrate was washed with 1M HCl (50 mL), aq NaHCO₃ saturated solution (3 x 50 mL) and brine (50 mL) and dried (Na₂SO₄). The mixture was filtered and the solvent was removed *in vacuo* to yield a dark brown oil which was purified by column chromatography (2:1 petroleum ether/ethyl acetate, *R_f*: 0.13): white solid (1.4g, 61%).

Mp: 140-141 °C. ¹H NMR (500 MHz, CDCl₃) δ 11.36 (s, 1H, OH), 9.76 (s, 1H), 7.46 (d, *J* = 8.6 Hz, 1H, Ar-H), 6.59 (dd, *J* = 8.6, 2.3 Hz, 1H, Ar-H), 6.54 (d, *J* = 2.3 Hz, 1H, Ar-H), 5.36 – 5.26 (m, 2H, H-1, H-2), 5.15 (m, 2H, H-3, H-4), 4.26 (dd, *J* = 12.3, 5.9 Hz, 1H, H-6), 4.17 (dd, *J* = 12.3, 2.5 Hz, 1H, H-6'), 3.91 (ddd, *J* = 9.9, 5.9, 2.5 Hz, 1H, H-5), 2.09, 2.05, 2.05, 2.03 (each s, 3H). ¹³C NMR (126 MHz, CDCl₃) δ 194.8 (HC=O), 170.6, 170.1, 169.4, 169.2 (each C=O), 164.0 (Ar-C), 163.2 (Ar-C), 135.4 (Ar-CH), 116.7 (Ar-C), 109.6 (Ar-CH), 103.6 (Ar-CH), 97.7 (C-1), 72.5 (C-2), 72.4 (C-5), 70.9 (C-3), 68.1 (C-6), 61.9 (C-4), 20.7, 20.68, 20.62, 20.61 (each OAc). IR (KBr disk): 3442, 2969, 2947, 2863, 1748, 1661, 1628, 1579, 1500, 1438, 1368, 1227, 1177, 1076, 1035, 979, 908, 802, 761 cm⁻¹. HRMS (ESI+): *m/z* calculated for C₂₁H₂₄O₁₂ + Na⁺ [*M* + Na⁺]: 491.1166. Found 491.1167. [α]_D²²: -6° (*c* = 0.5, CH₂Cl₂). NMR data is in agreement with that reported in the literature.ⁱⁱⁱ

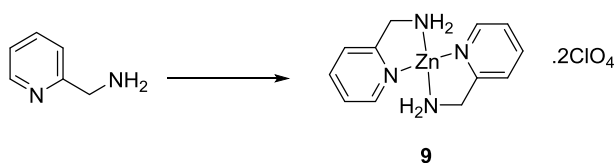
4.5 Synthesis of 2-hydroxy-4-(2-hydroxyethoxy)benzaldehyde **5c**.



2, 4-dihydroxybenzaldehyde (1 g, 7.2 mmol), 2-chloroethanol (0.97 mL, 14.4 mmol), DBU (1.07 mL, 7.2 mmol) and sodium iodide (0.539 g, 3.6 mmol) were dissolved in isopropyl alcohol (25 mL). The mixture was sealed in a microwave tube and heated under microwave irradiation to 150 °C for 4 h. The solvent was removed *in vacuo* and the residue was dissolved in ethyl acetate (50 mL) and washed with aq NaHCO₃ saturated solution (50 mL), water (3 x 50 mL) and brine (50 mL). The organic layer was dried (Na₂SO₄). The mixture was filtered and the solvent was removed *in vacuo* to yield a brown oil which was purified by column chromatography (2:1 petroleum ether/ethyl acetate, *R_f*: 0.43): white solid (0.996 g, 76%).

Mp: 76-77 °C. ^1H NMR (500 MHz, CDCl_3) δ 11.47 (s, 1H, Ar-OH), 9.72 (s, 1H, C(=O)H), 7.44 (d, J = 8.7 Hz, 1H, Ar-H), 6.57 (dd, J = 8.7, 2.3 Hz, 1H, Ar-H), 6.44 (d, J = 2.3 Hz, 1H), 4.15 – 4.12 (m, 2H, ArOCH₂), 3.99 (m, J = 3.8 Hz, 2H, CH₂OH), 2.04 (s, 1H, CH₂OH). ^{13}C NMR (126 MHz, CDCl_3) δ 194.5 (HC=O), 165.8 (Ar-C), 164.4 (Ar-C), 135.4 (Ar-CH), 115.4 (Ar-C), 108.6 (Ar-CH), 101.8 (Ar-CH), 69.7 (ArOCH₂), 61.1 (CH₂OH). IR (KBr disk): 3462, 3446, 2959, 2921, 2865, 1804, 1648, 1495, 1232, 1168, 1047 cm^{-1} . HRMS (ESI+): m/z calculated for $\text{C}_9\text{H}_{10}\text{O}_4 + \text{H}^+$ [$\text{M} + \text{H}^+$]: 183.0657. Found: 183.0661. Elemental analysis calculated (%) for $\text{C}_9\text{H}_{10}\text{O}_4$: C 59.34, H 5.53. Found: C 58.98, H 5.55. NMR data is in agreement with that reported in the literature.ⁱ

4.6 Synthesis of bis(2-picolylamine)zinc perchlorate **9**.

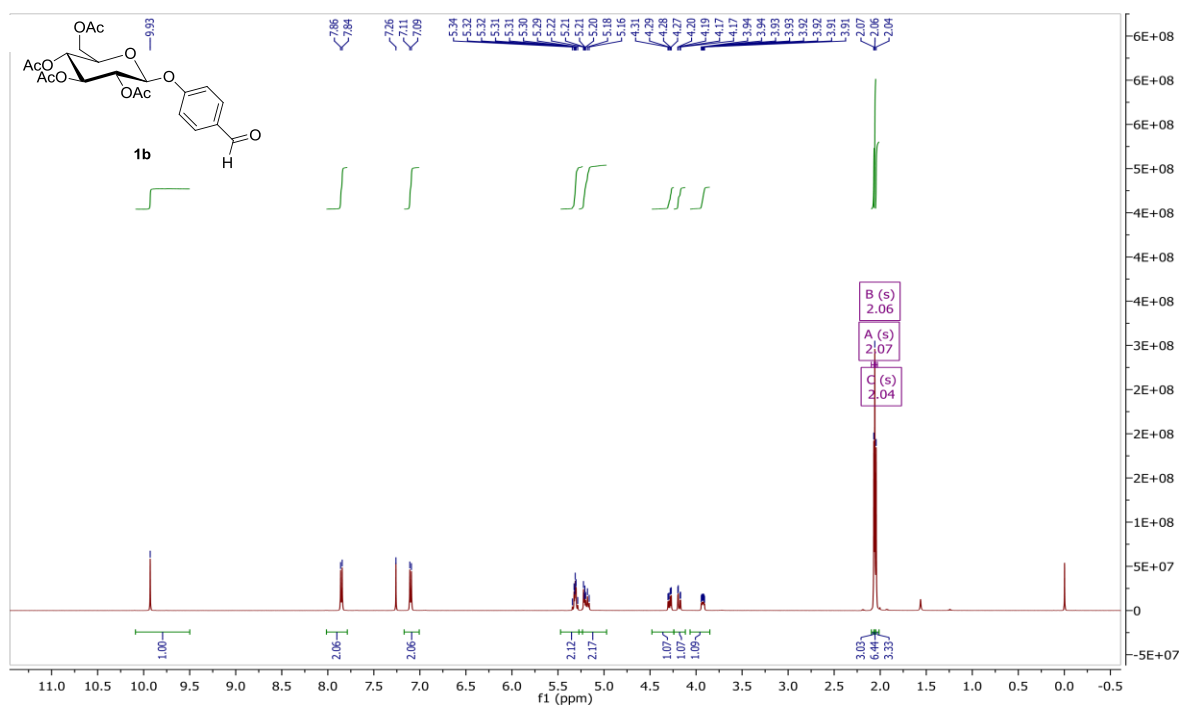


$\text{Zn}(\text{ClO}_4)_2 \cdot 6\text{H}_2\text{O}$ (723 mg, 1.9 mmol) and 2-picolylamine (0.4 mL, 3.8 mmol) were stirred at rt in ethanol (20 mL) for 4 h and cooled on ice for 30 min. This yielded a white precipitate which was collected by vacuum filtration, washed with cold ethanol and dried under vacuum: white solid (855 mg, 94%).

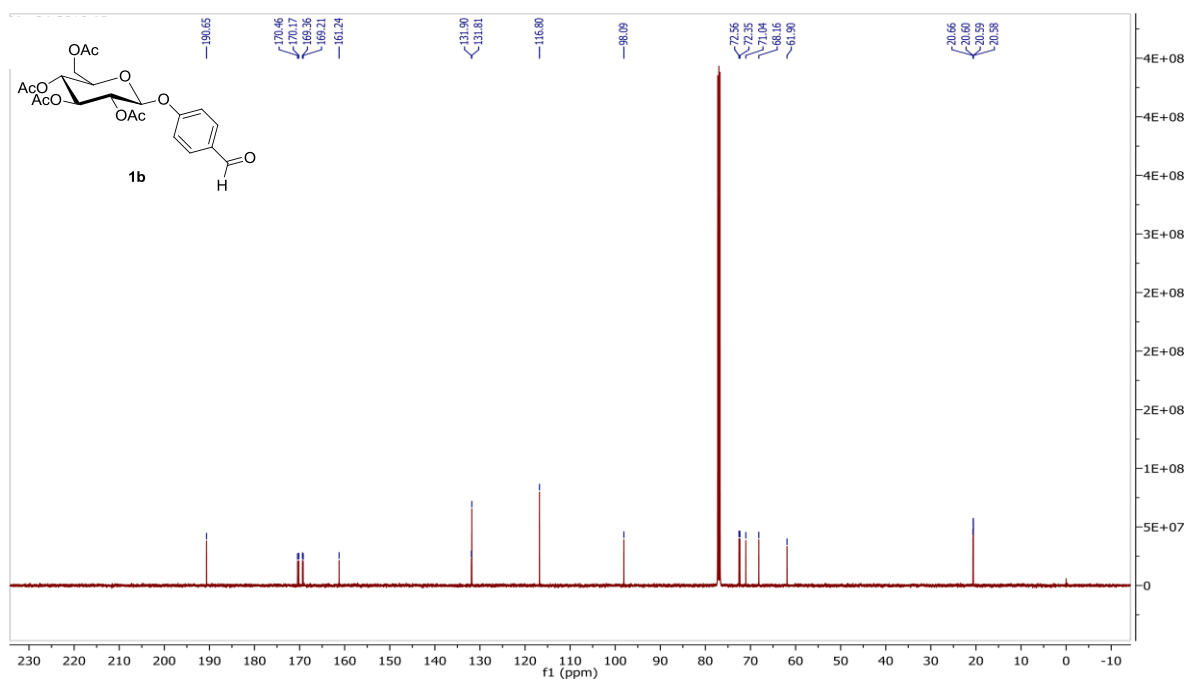
Mp: Compound decomposes at 245 °C. ^1H NMR (500 MHz, DMSO) δ 8.30 (d, J = 2.9 Hz, 2H, Pyr-H), 8.05 (t, J = 7.2 Hz, 2H, Pyr-H), 7.59 (d, J = 7.9 Hz, 2H, Pyr-H), 7.56 – 7.50 (m, 2H, Pyr-H), 4.08 (s, 4H, CH₂), 3.91 (s, 4H, NH₂). ^{13}C NMR (126 MHz, DMSO) δ 157.4 (Pyr-C), 146.8 (Pyr-CH), 139.7 (Pyr-CH), 123.8 (Pyr-CH), 123.5 (Pyr-CH), 42.6 (CH₂). IR (KBr disk): 3439, 3281, 3204, 3133, 2912, 1603, 1590, 1569, 1487, 1439, 1383, 1334, 1294, 1141, 1114, 1090, 1032, 1017, 940, 772, 636, 626 cm^{-1} . Elemental analysis calculated (%) for $\text{C}_{12}\text{H}_{16}\text{N}_4\text{Cl}_2\text{O}_8\text{Zn}$: C 29.99, H 3.36, N 11.6. Found: C 29.51, H, 3.32, N 11.45.

5. Spectroscopic data

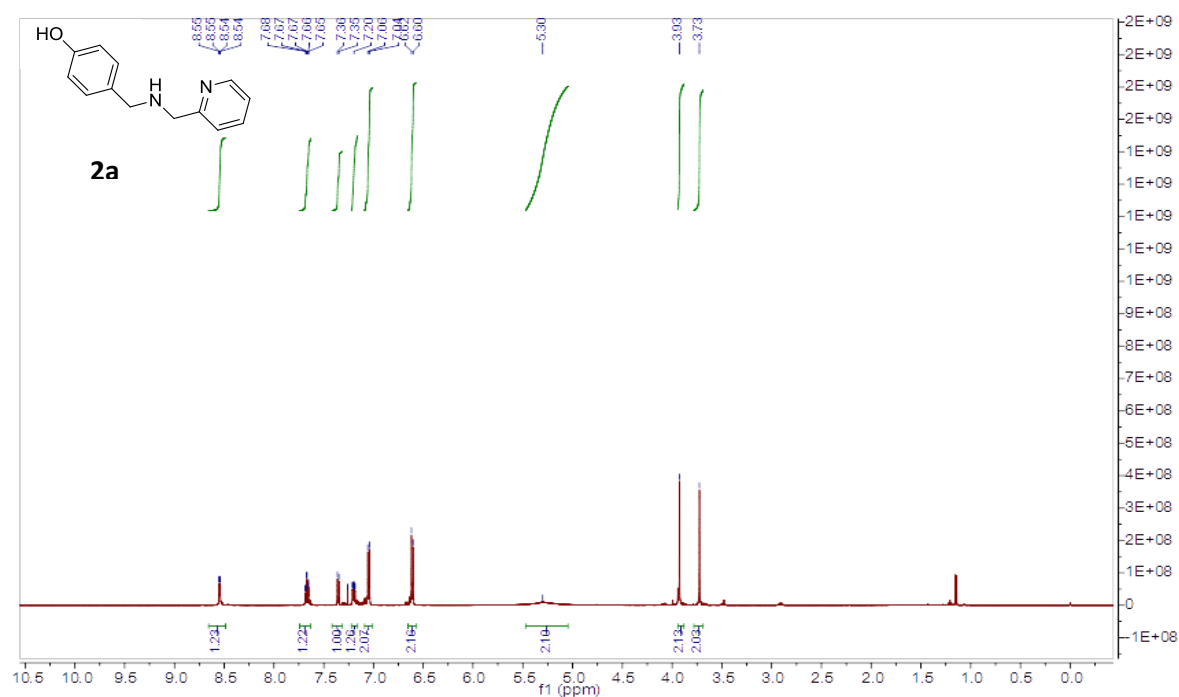
5.1 ^1H NMR spectrum of 4-(2,3,4,6-tetra-*O*-acetyl- β -D-glucopyranosyloxy)benzaldehyde **1b**



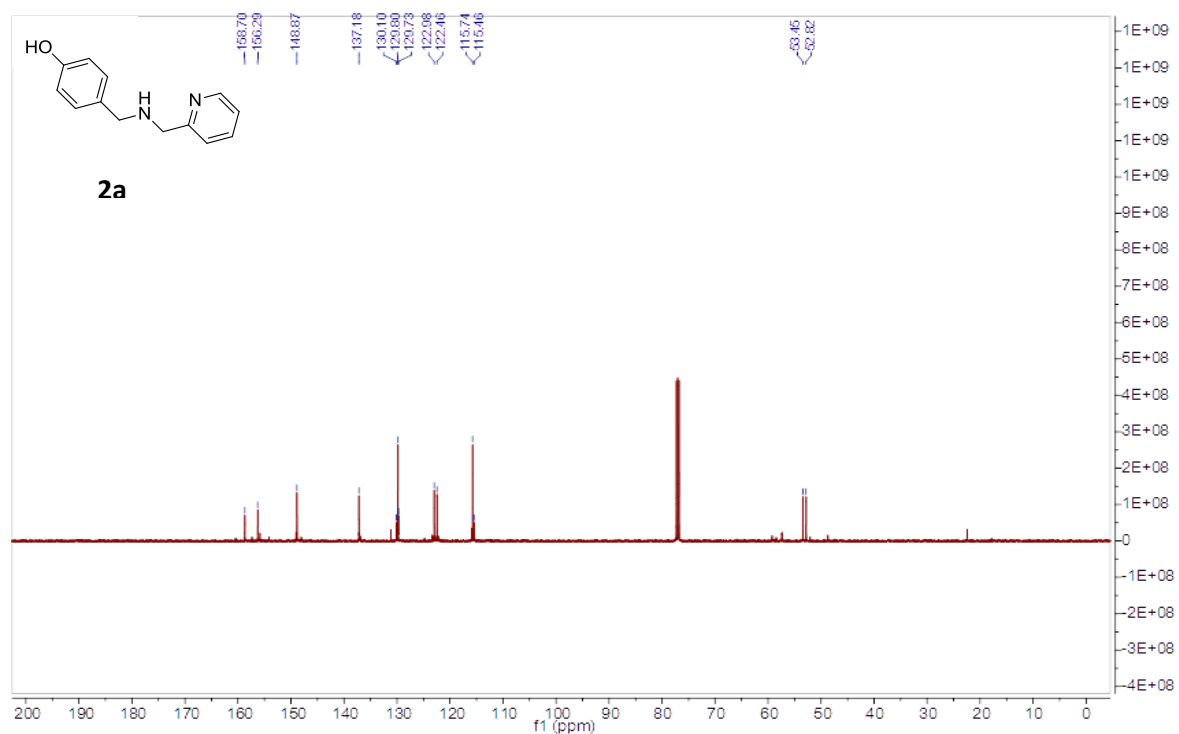
5.2 ^{13}C NMR spectrum of 4-(2,3,4,6-tetra-*O*-acetyl- β -D-glucopyranosyloxy)benzaldehyde **1b**



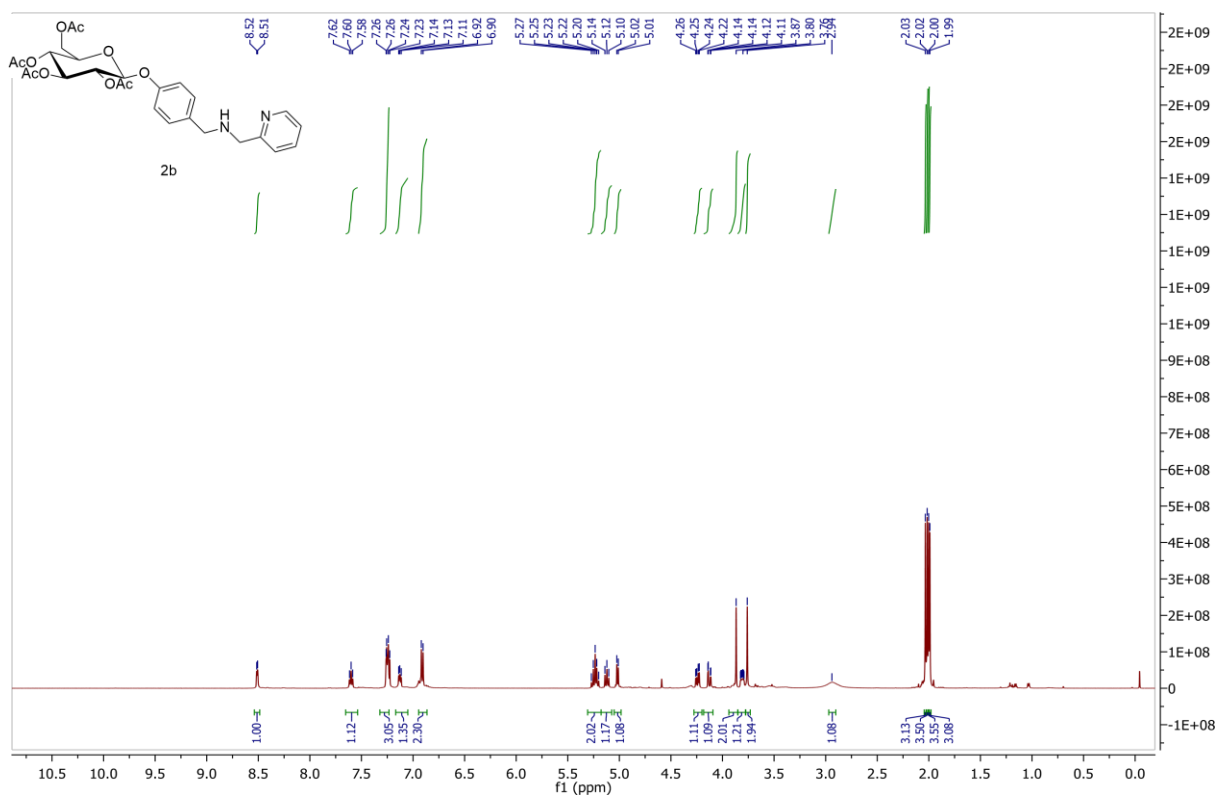
5.3 ^1H NMR spectrum of *N*-[4-(hydroxyphenyl)methyl]-2-pyridinemethamine **2a**



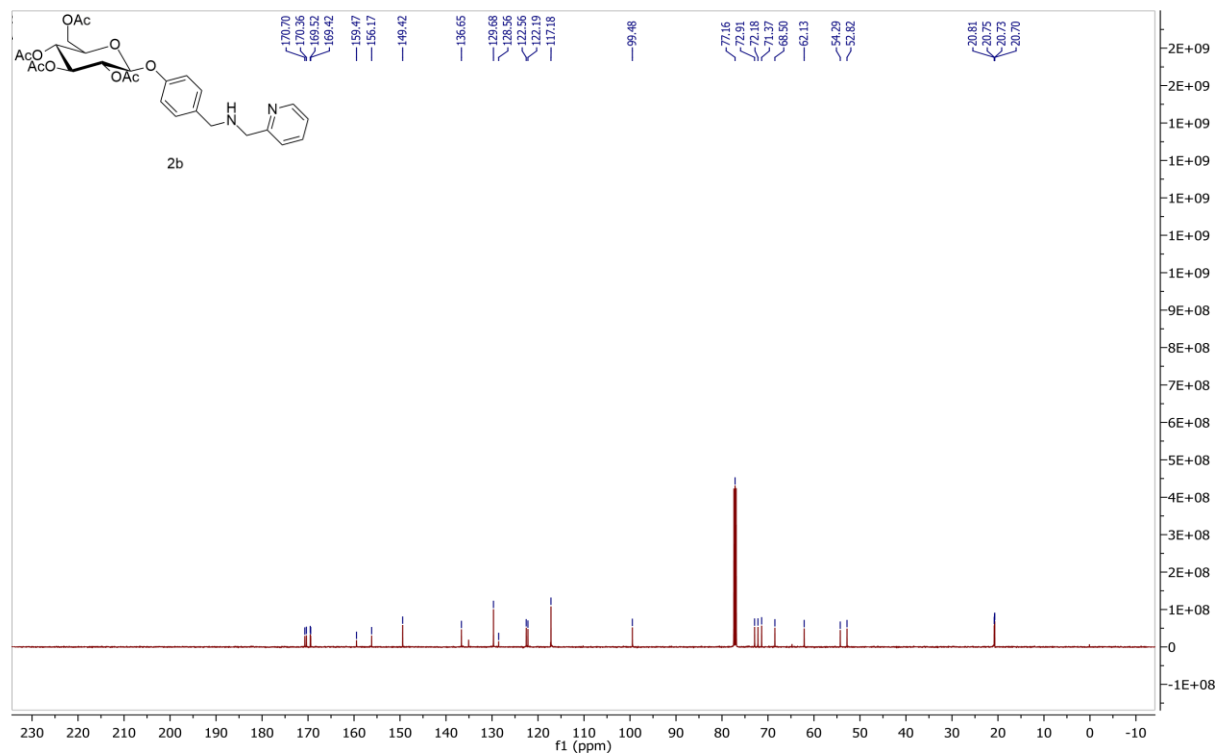
5.4 ^{13}C NMR spectrum of *N*-[4-(hydroxyphenyl)methyl]-2-pyridinemethamine **2a**



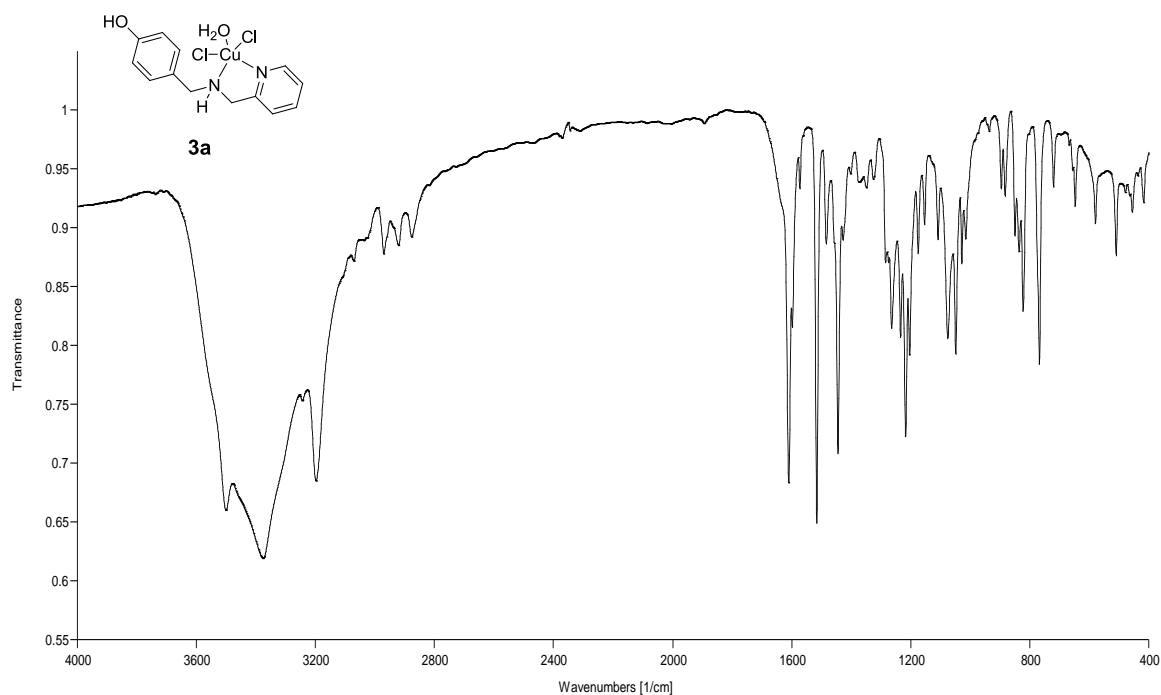
5.5 ¹H NMR spectrum of N-{[4-(2,3,4,6-tetra-O-acetyl-β-D-glucopyranosyloxy)phenyl]methyl}-2-pyridinemethamine **2b**



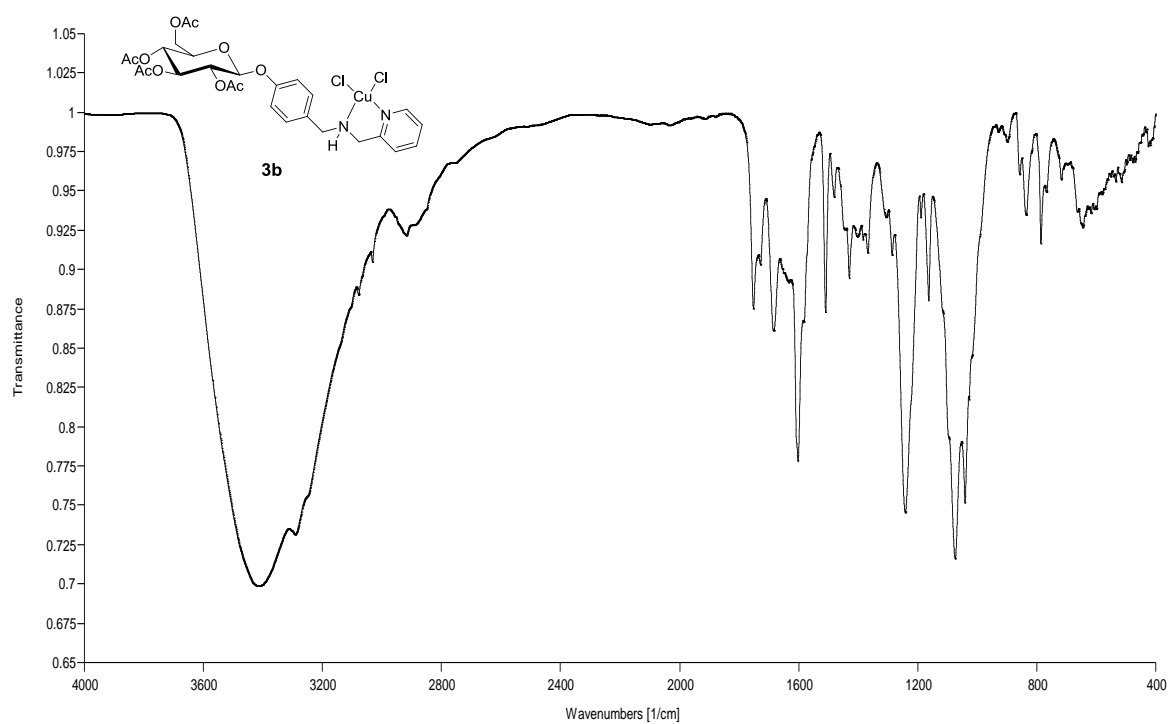
5.6 ¹³C NMR spectrum of N-[[4-(2,3,4,6-tetra-O-acetyl-β-D-glucopyranosyloxy)phenyl]methyl]-2-pyridinemethamine **2b**



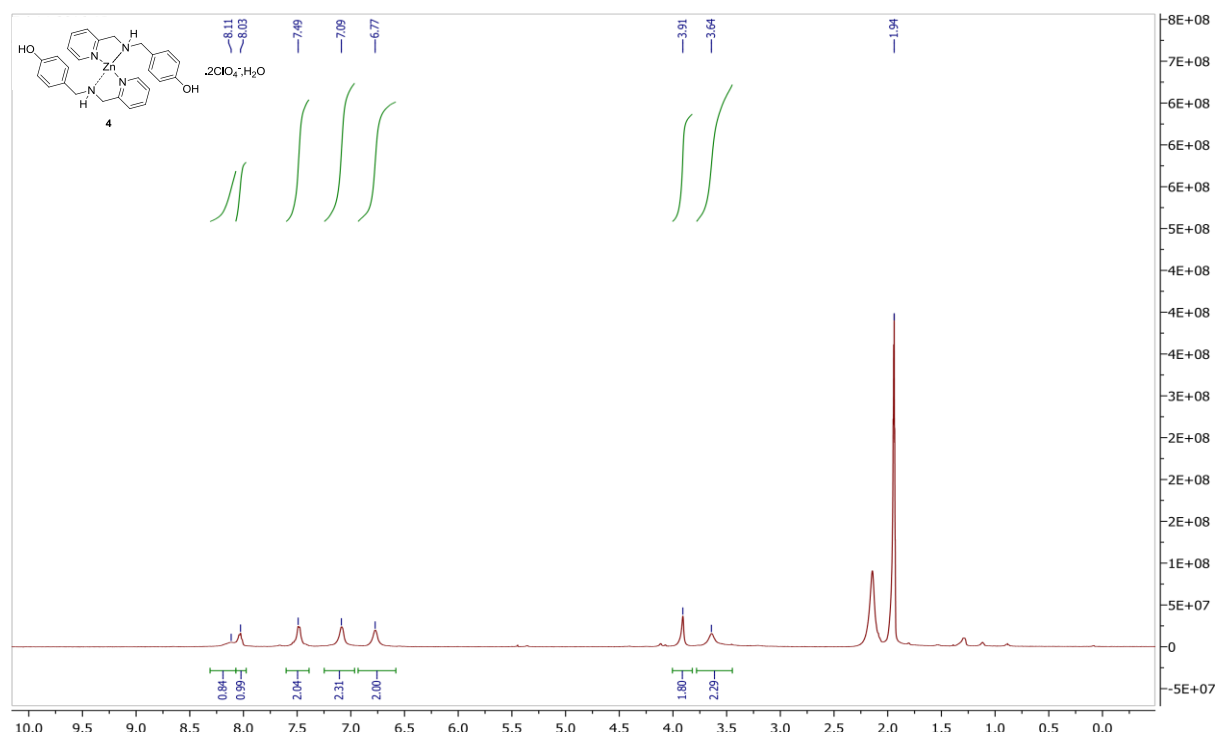
5.7 FTIR spectrum of *cis*-aquadichloro(*N*-[4-(hydroxyphenyl)methyl]-2-pyridinemethamine)copper **3a**



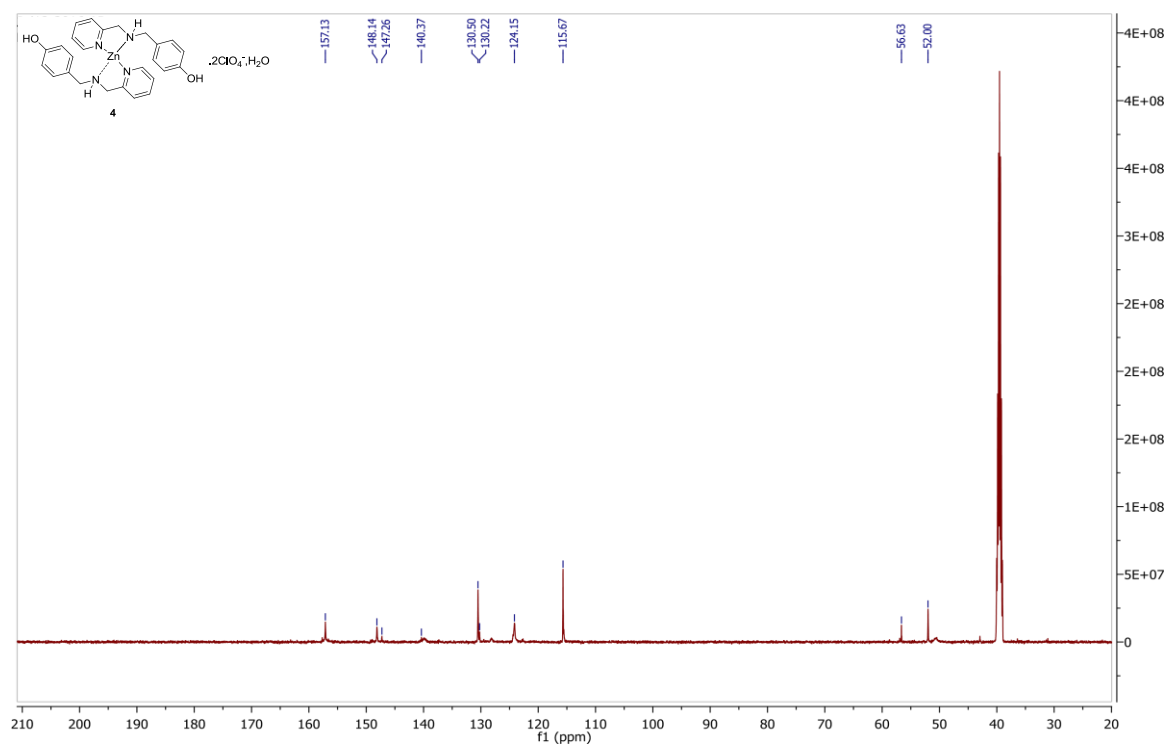
5.8 FTIR spectrum of *cis*-dichloro(*N*-{[4-(2,3,4,6-tetra-*O*-acetyl- β -D-glucopyranosyloxy)phenyl]methyl}-2-pyridinemethamine)copper **3b**



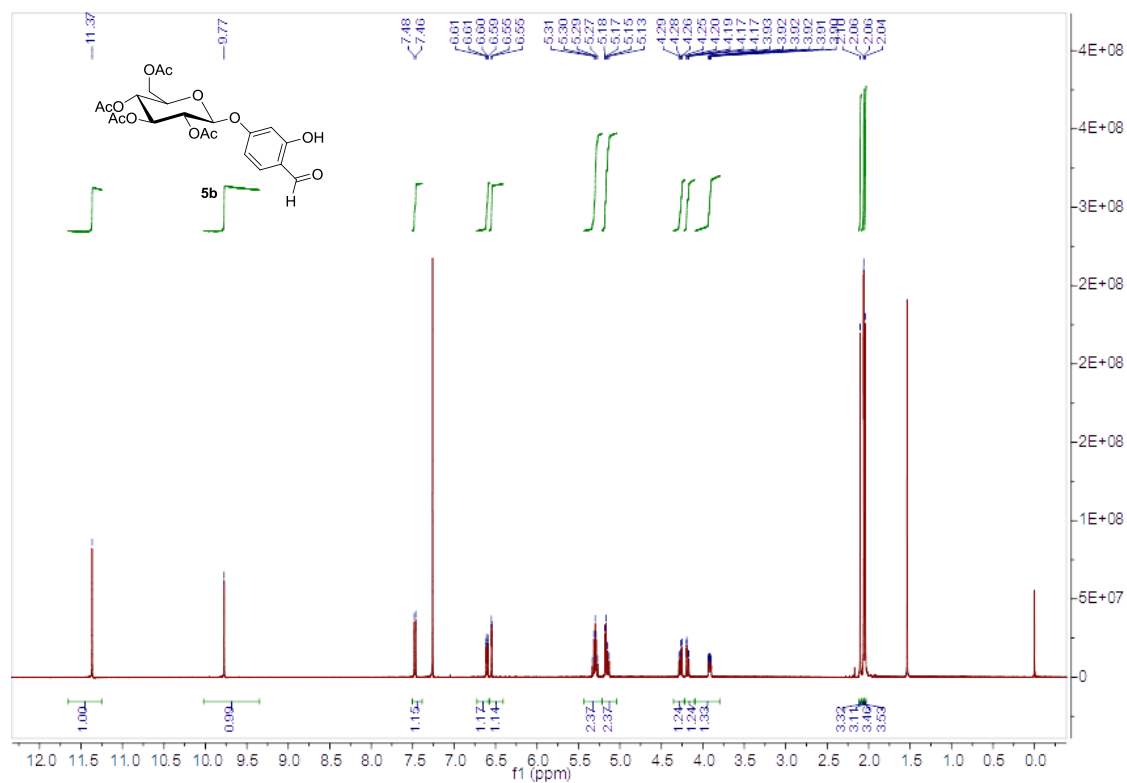
5.9 ^1H NMR spectrum of bis(*N*-[4-(hydroxyphenyl)methyl]-2-pyridinemethamine)zinc perchlorate monohydrate **4**



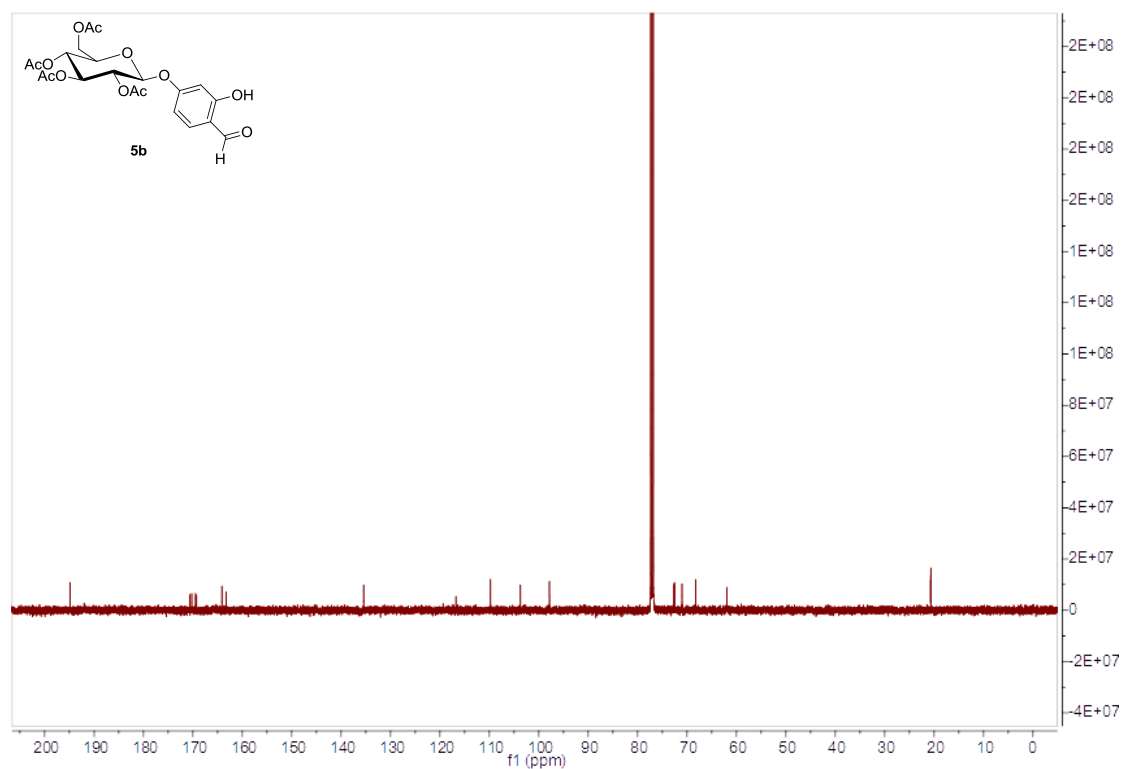
5.10 ^{13}C NMR spectrum of bis(*N*-[4-(hydroxyphenyl)methyl]-2-pyridinemethamine)zinc perchlorate monohydrate **4**



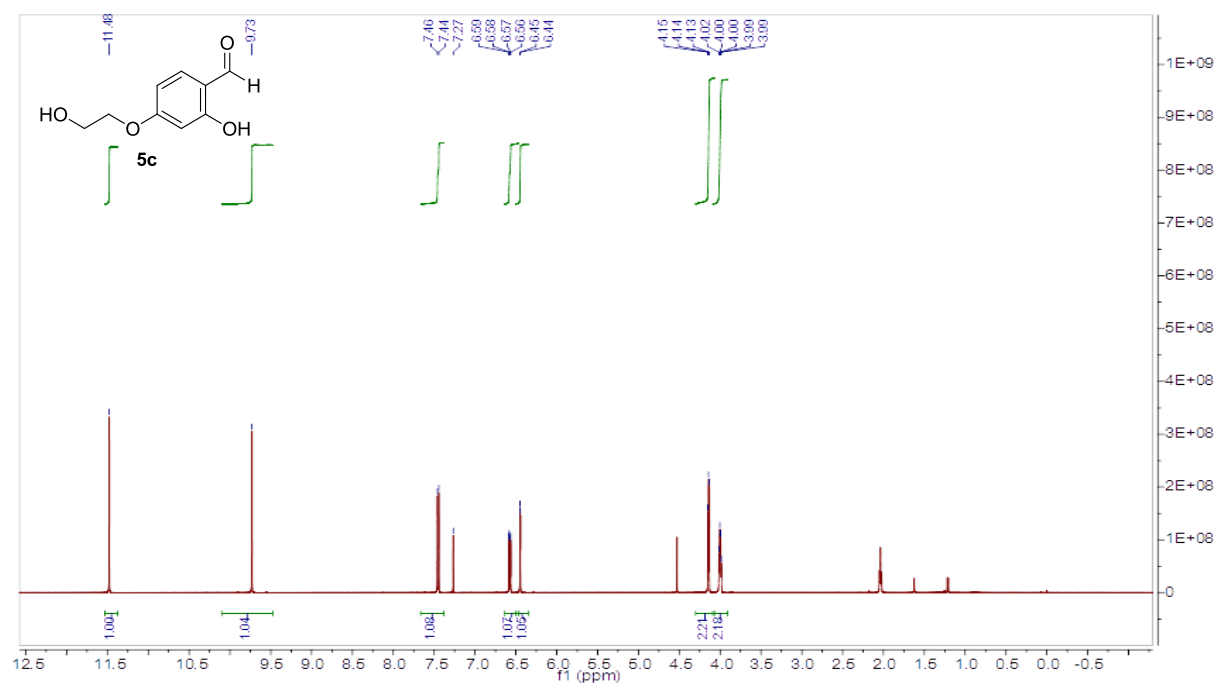
5.11 ^1H NMR spectrum of 2-hydroxy-4-(2,3,4,6-tetra-*O*-acetyl- β -D-glucopyranosyloxy)benzaldehyde **5b**



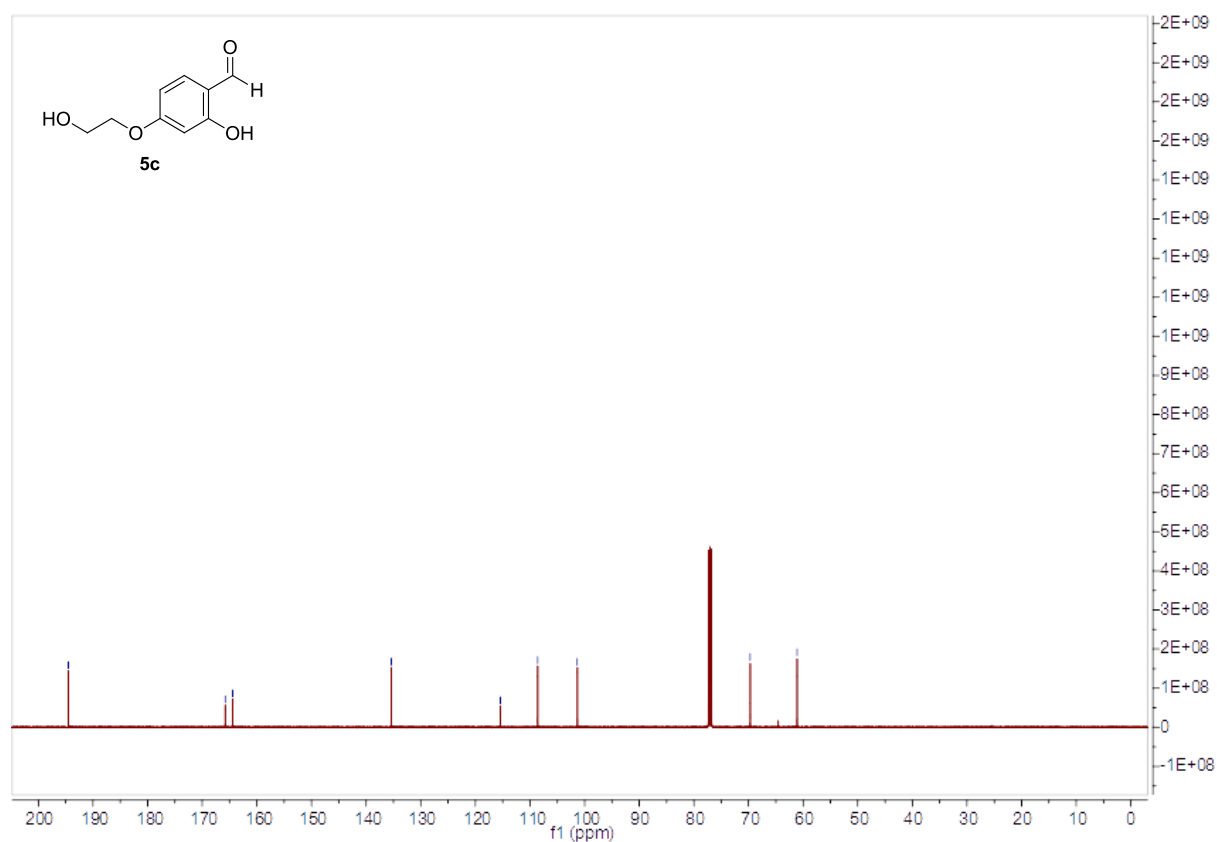
5.12 ^{13}C NMR spectrum of 2-hydroxy-4-(2,3,4,6-tetra-*O*-acetyl- β -D-glucopyranosyloxy)benzaldehyde **5b**



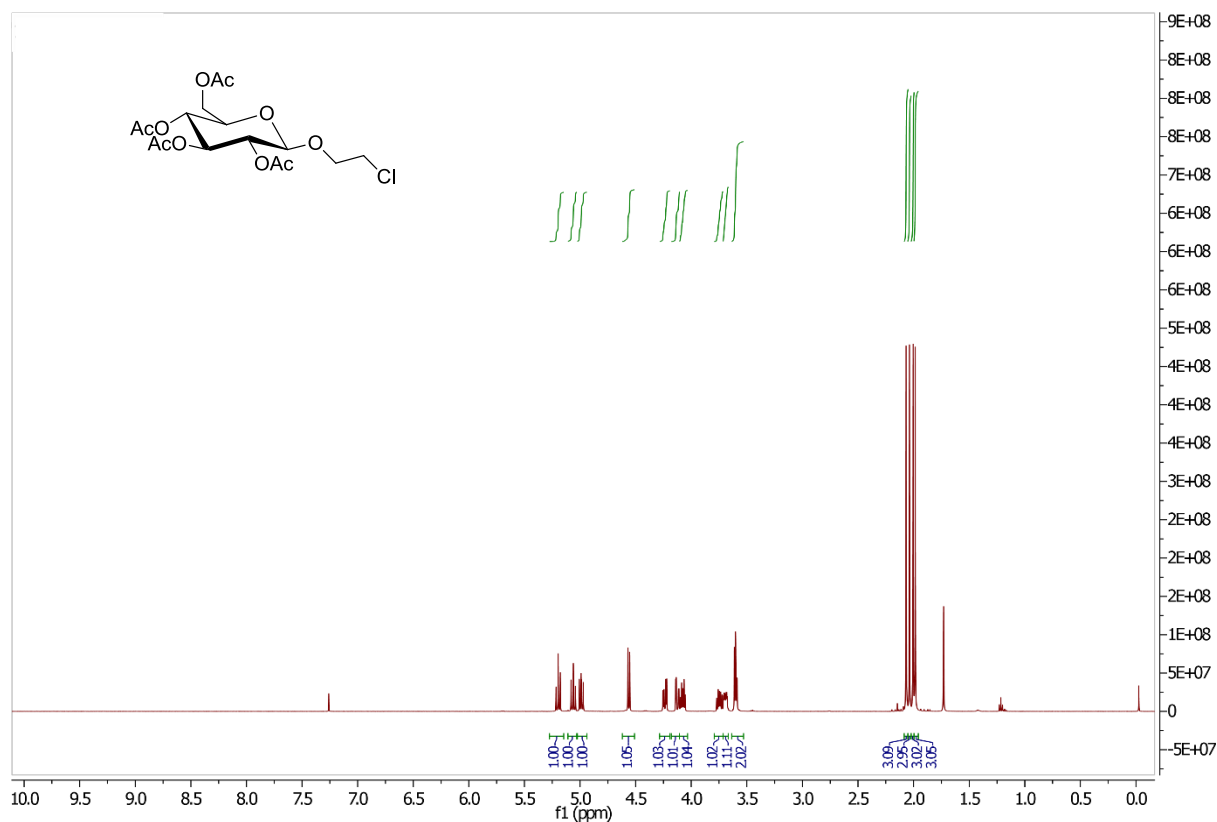
5.13 ^1H NMR spectrum of 2-hydroxy-4-(2-hydroxyethoxy)benzaldehyde **5c**



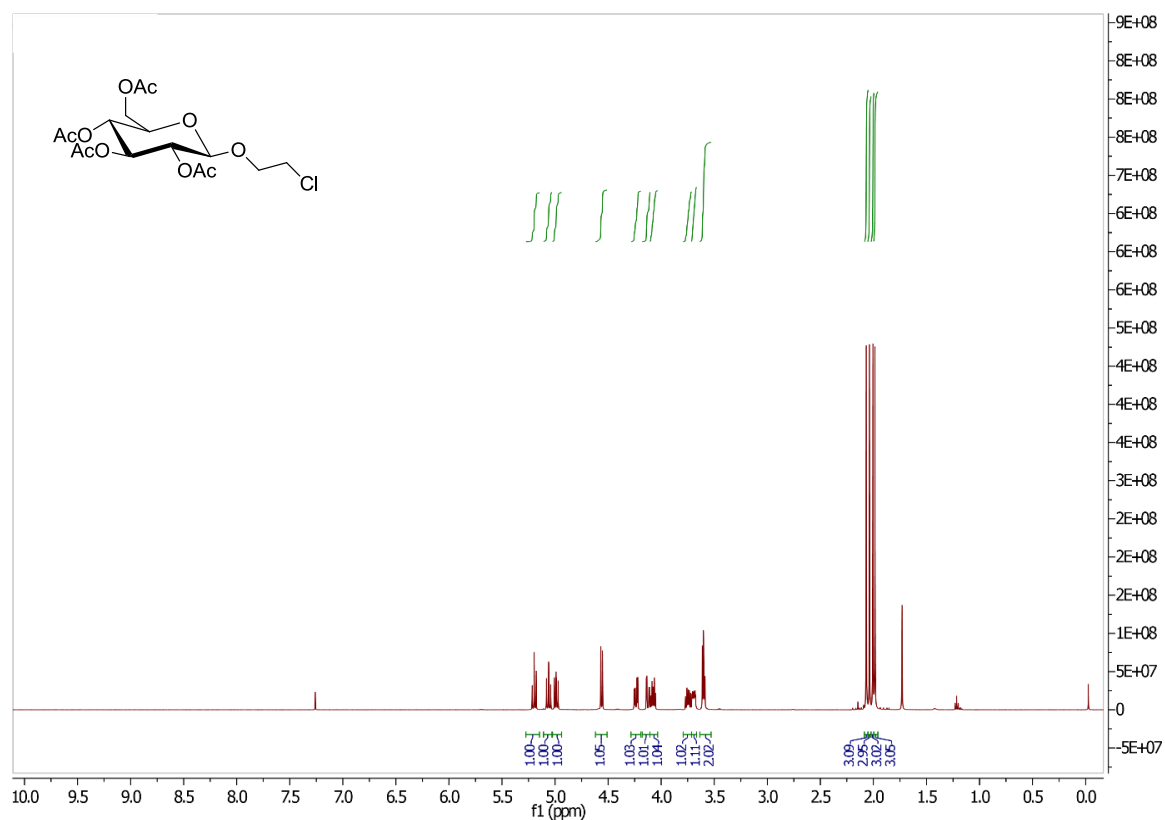
5.14 ^{13}C NMR spectrum of 2-hydroxy-4-(2-hydroxyethoxy)benzaldehyde **5c**



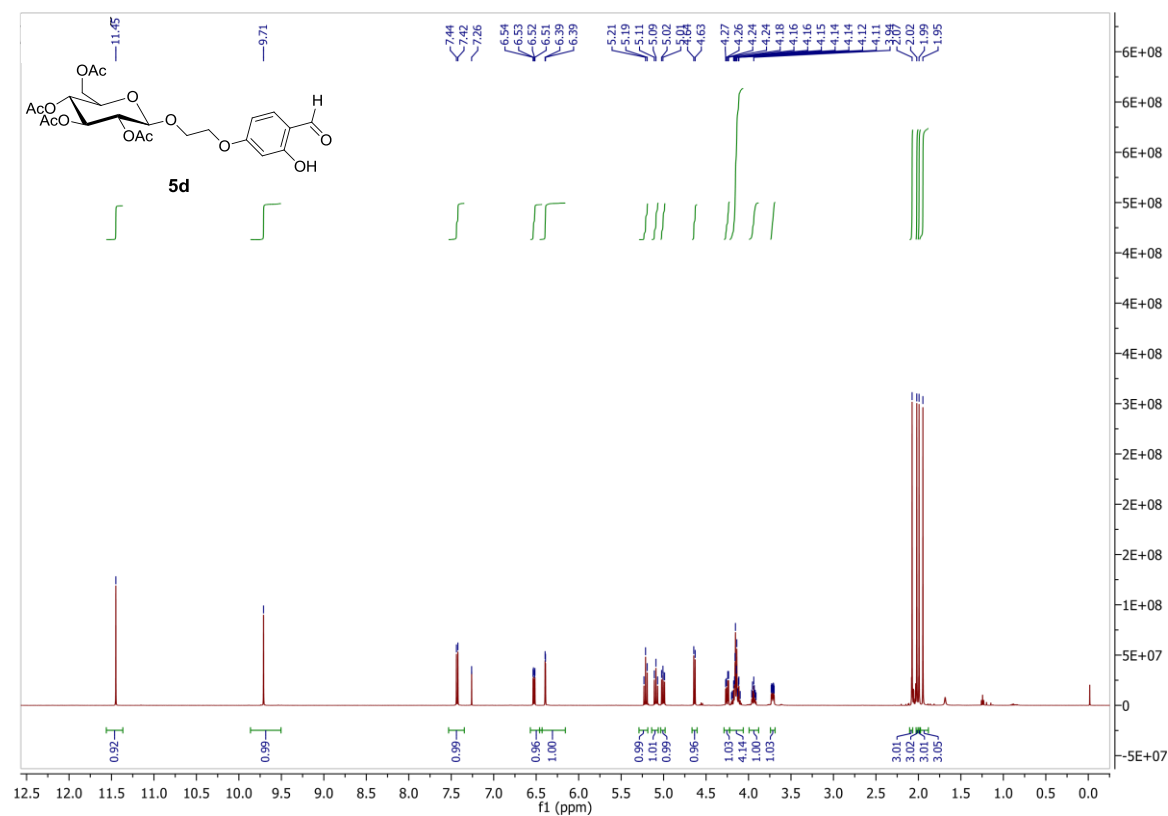
5.15 ^1H NMR spectrum of 2-chloroethyl 2,3,4,6-tetra-*O*-acetyl- β -D-glucopyranoside (starting material for the synthesis of **5d**).



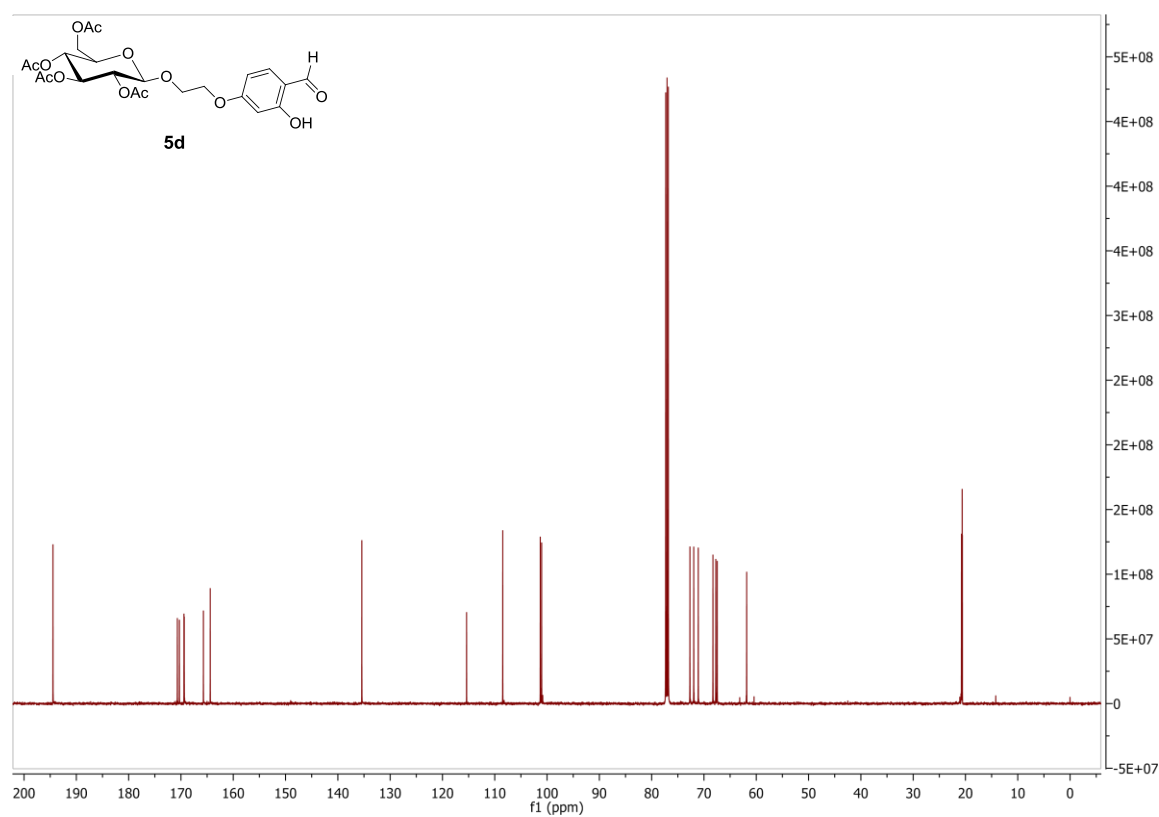
5.16 ^{13}C NMR spectrum of 2-chloroethyl 2,3,4,6-tetra-*O*-acetyl- β -D-glucopyranoside (starting material for the synthesis of **5d**).



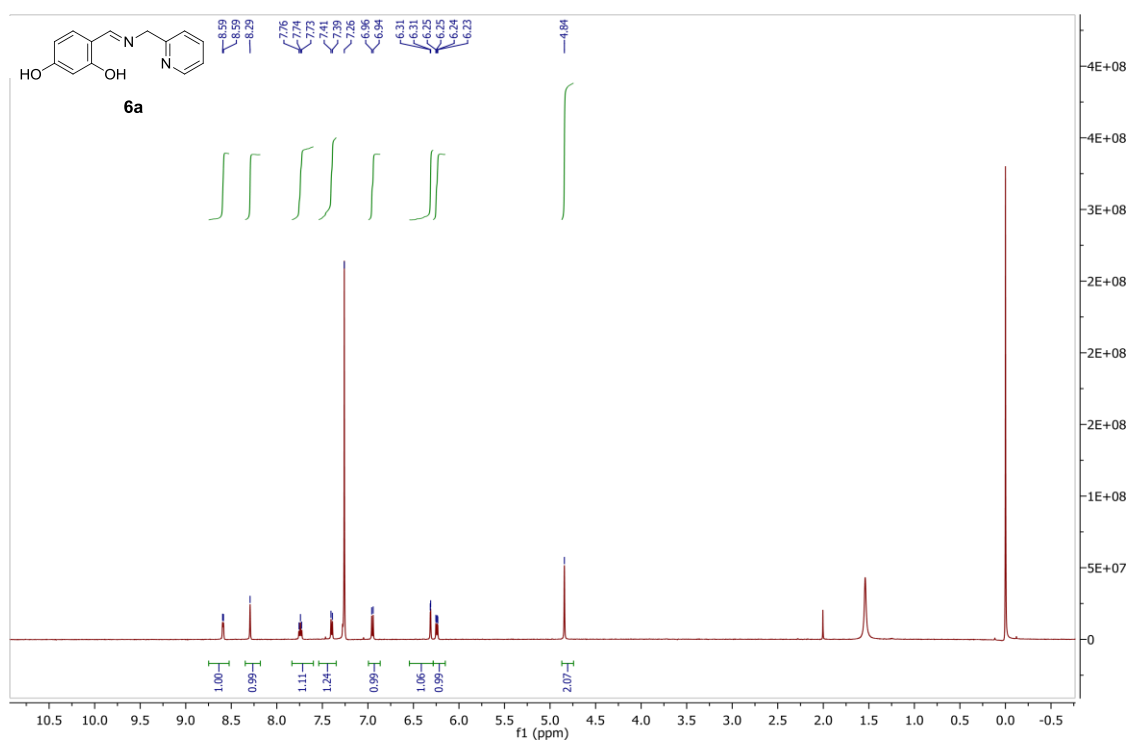
5.17 ^1H NMR spectrum of 2-hydroxy-4-[2-(2,3,4,6-tetra-*O*-acetyl- β -D-glucopyranosyloxy)ethoxy]benzaldehyde **5d**



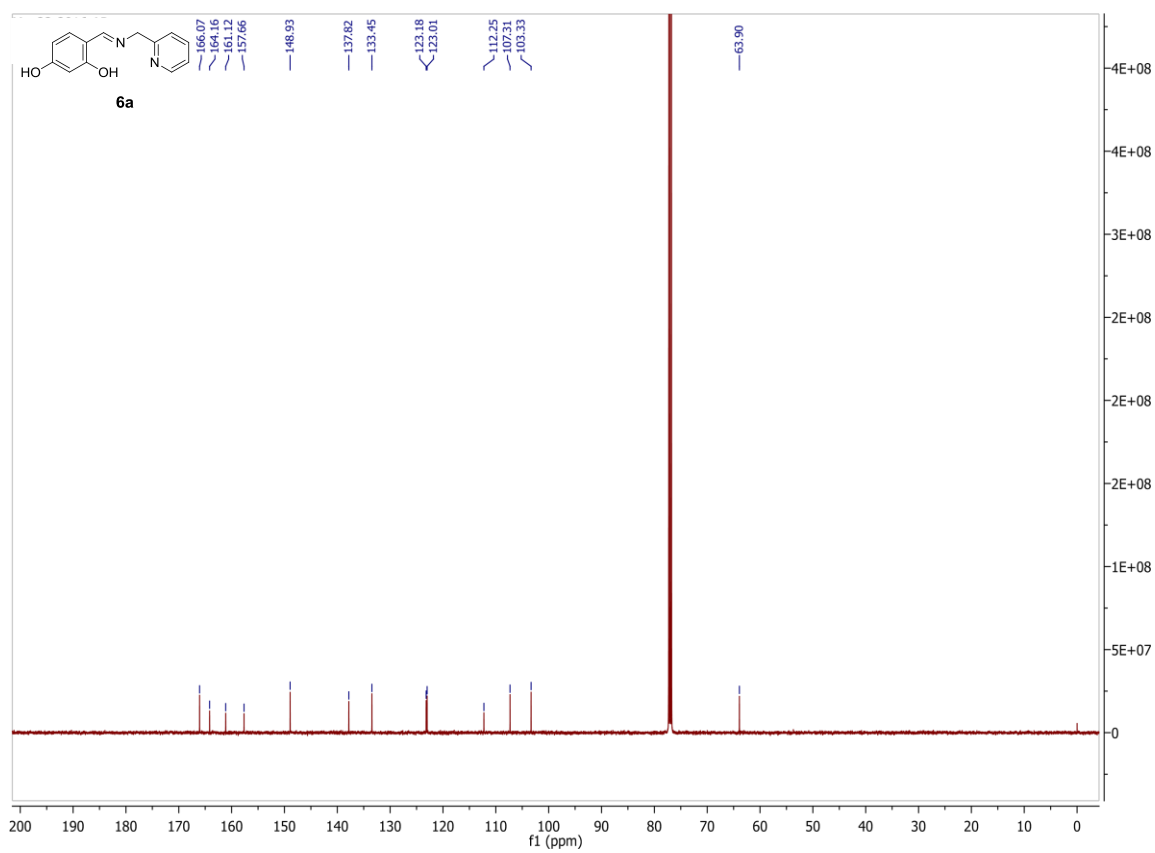
5.18 ^{13}C NMR spectrum of 2-hydroxy-4-[2-(2,3,4,6-tetra-*O*-acetyl- β -D-glucopyranosyloxy)ethoxy]benzaldehyde **5d**



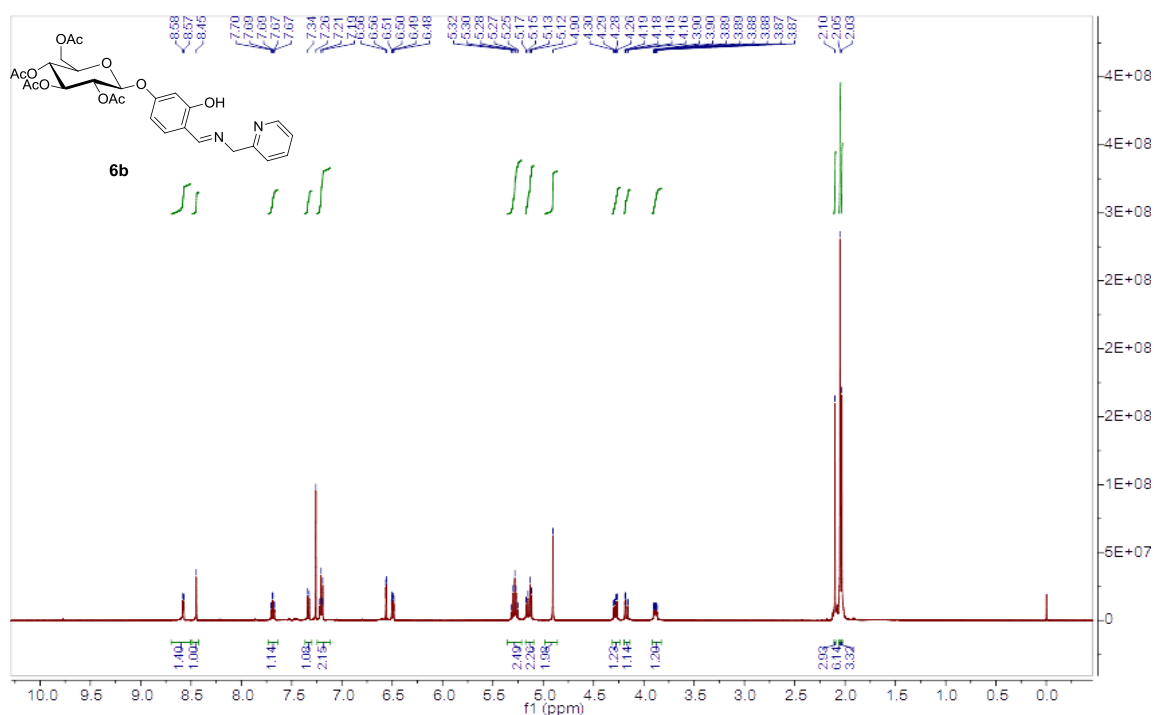
5.19 ^1H NMR spectrum of 4-[[2-methylpyridinyl]-E-imino]methyl}-benzene-1,3-diol **6a**



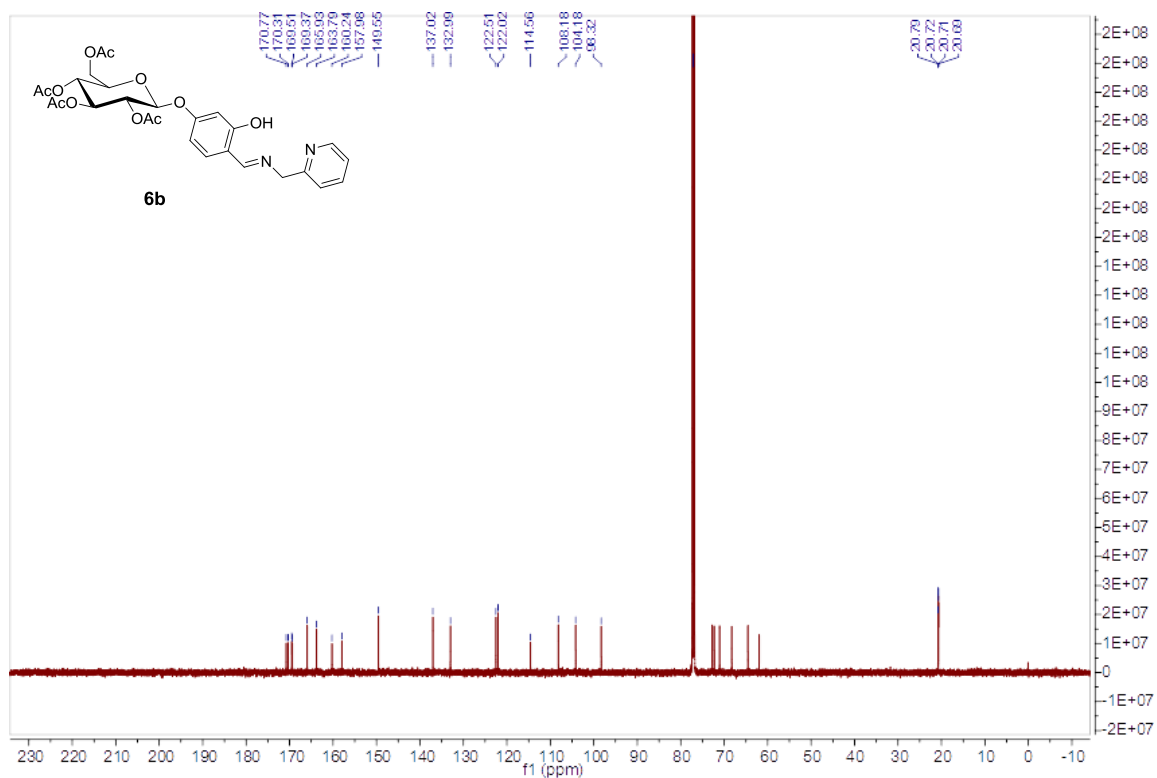
5.20 ^{13}C NMR spectrum of 4-[[2-methylpyridinyl]-E-imino]methyl}-benzene-1,3-diol **6a**



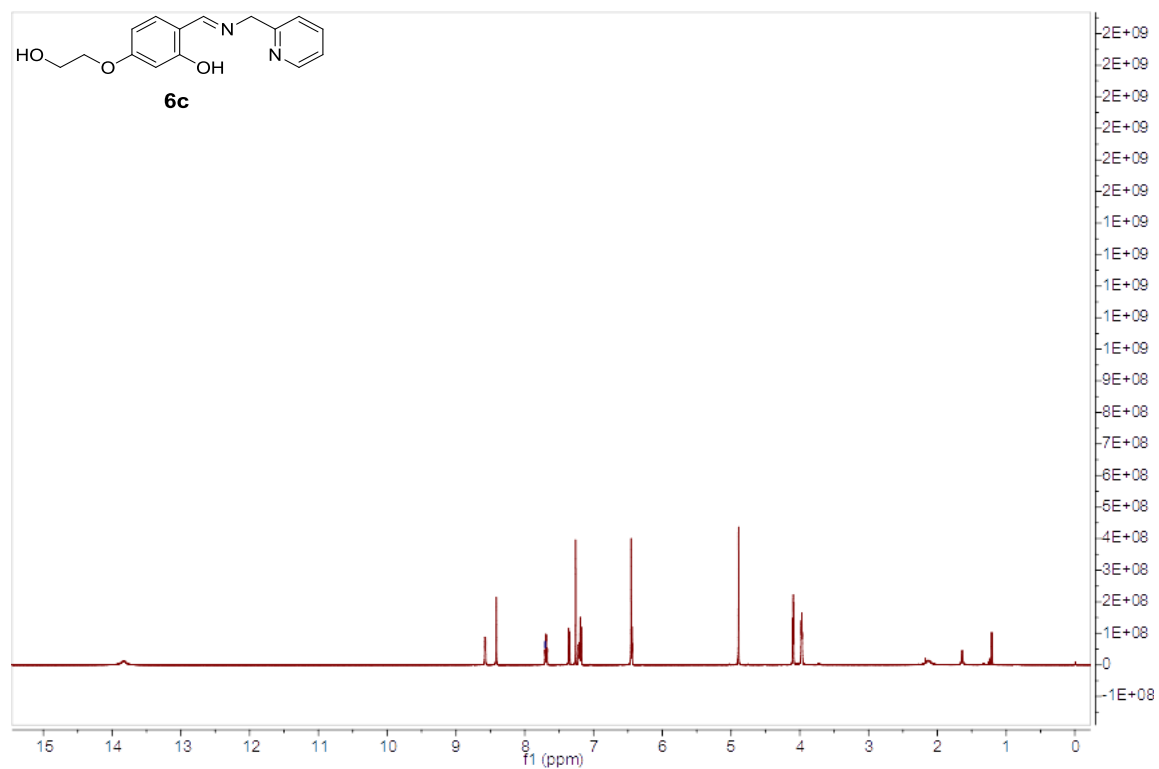
5.21 ¹H NMR spectrum of 5-(2,3,4,6-tetra-O-acetyl-β-D-glucopyranosyloxy)-2-[(2-methylpyridinyl)-E-imino]methylphenol **6b**



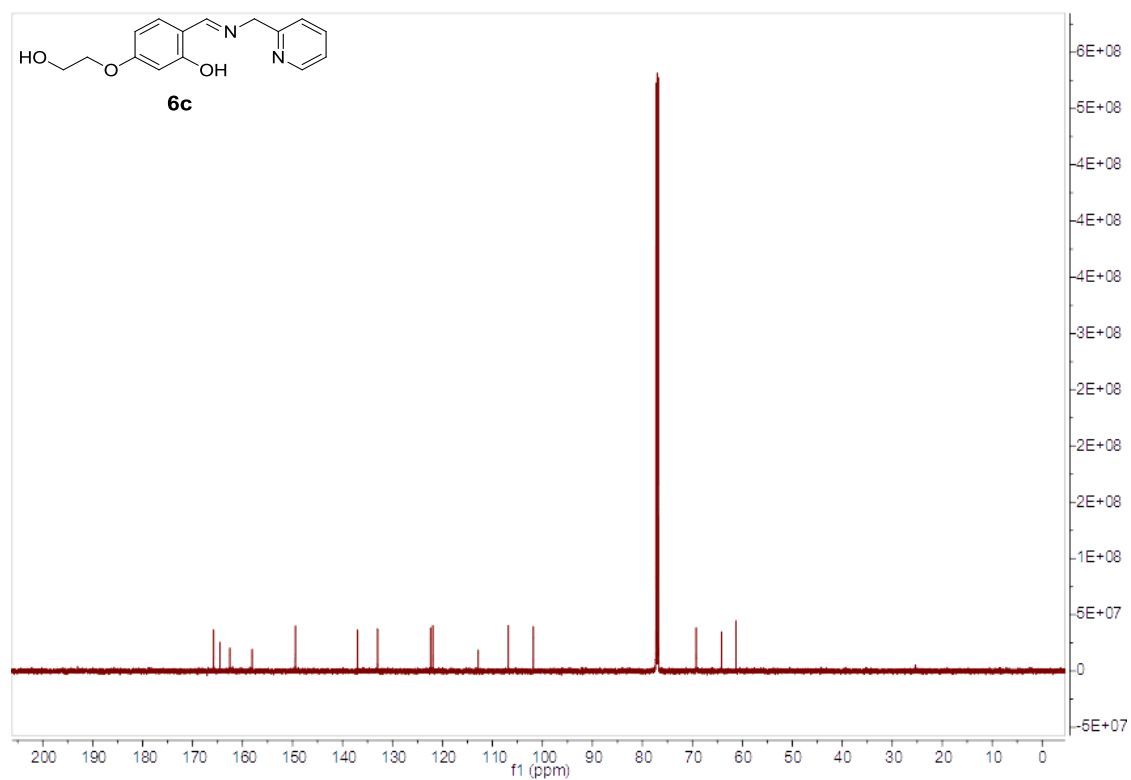
5.22 ¹³C NMR spectrum of 5-(2,3,4,6-tetra-O-acetyl-β-D-glucopyranosyloxy)-2-[(2-methylpyridinyl)-E-imino]methylphenol **6b**



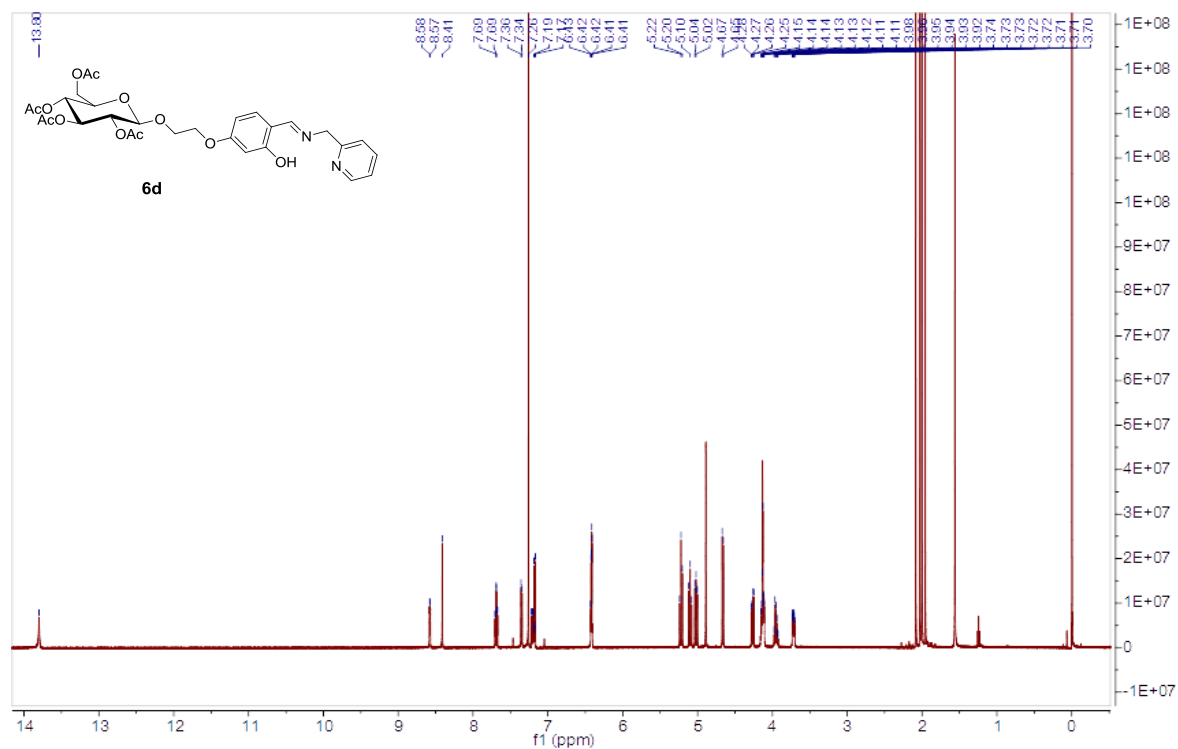
5.23 ^1H NMR spectrum of 5-(2-hydroxyethoxy)-2-[(2-methylpyridinyl)-E-imino]methyl}phenol **6c**



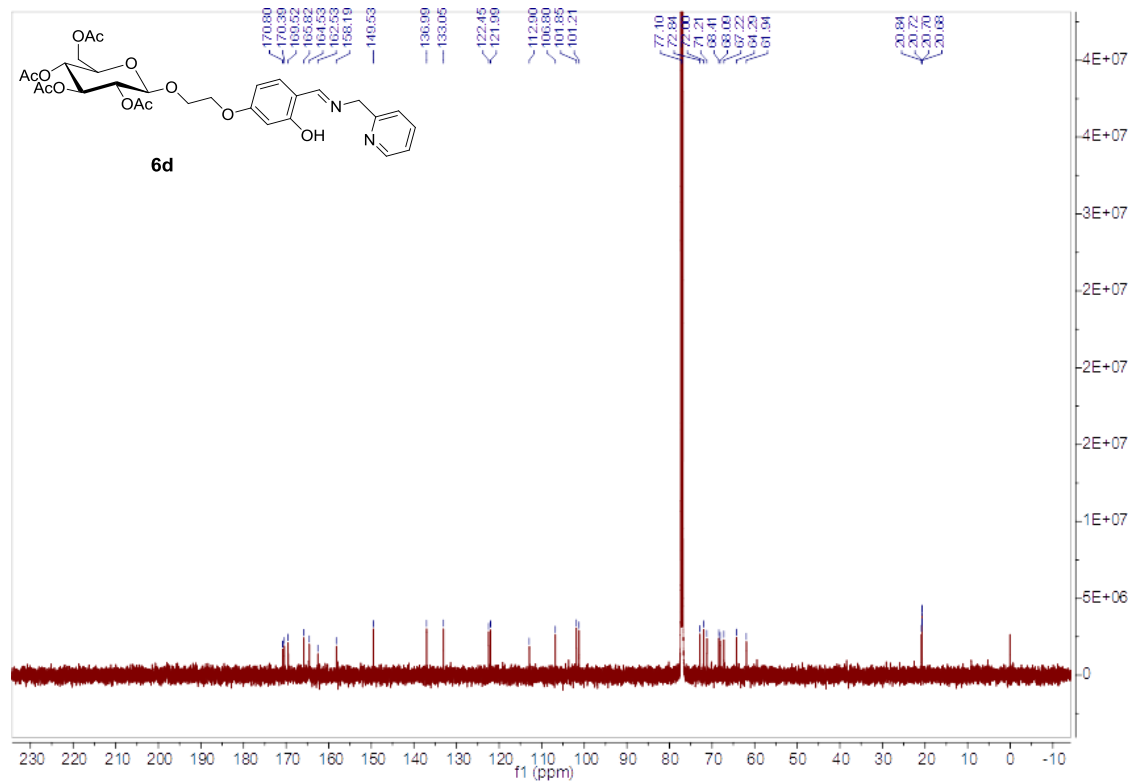
5.24 ^{13}C NMR spectrum of 5-(2-hydroxyethoxy)-2-[(2-methylpyridinyl)-E-imino]methyl}phenol **6c**



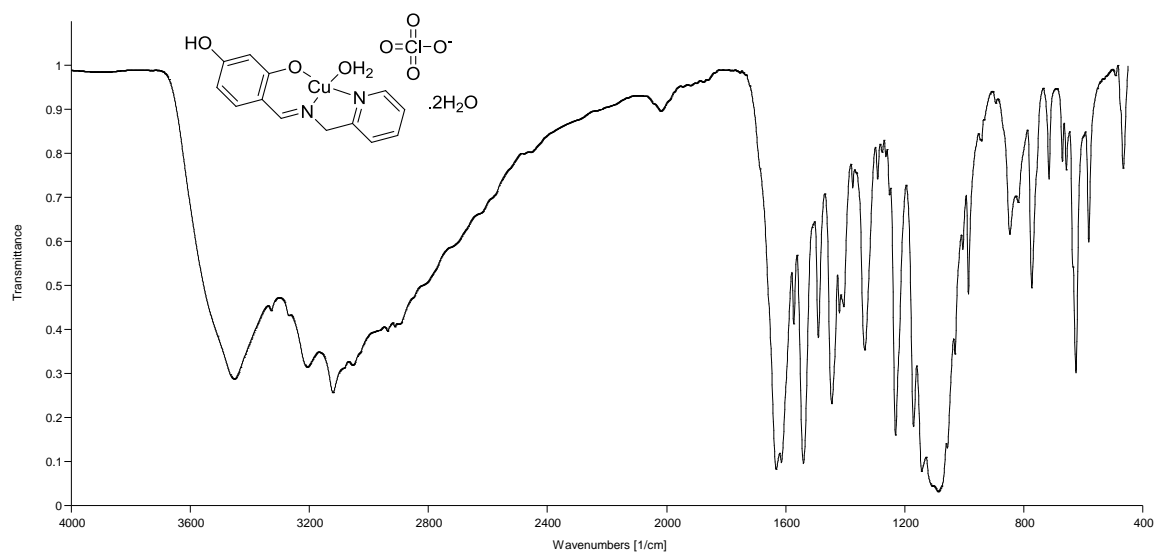
5.25¹H NMR spectrum of 5-[2-(2,3,4,6-tetra-O-acetyl-β-D-glucopyranosyloxy)ethoxy)-2-{[(2-methylpyridinyl)-E-imino]methyl}phenol **6d**



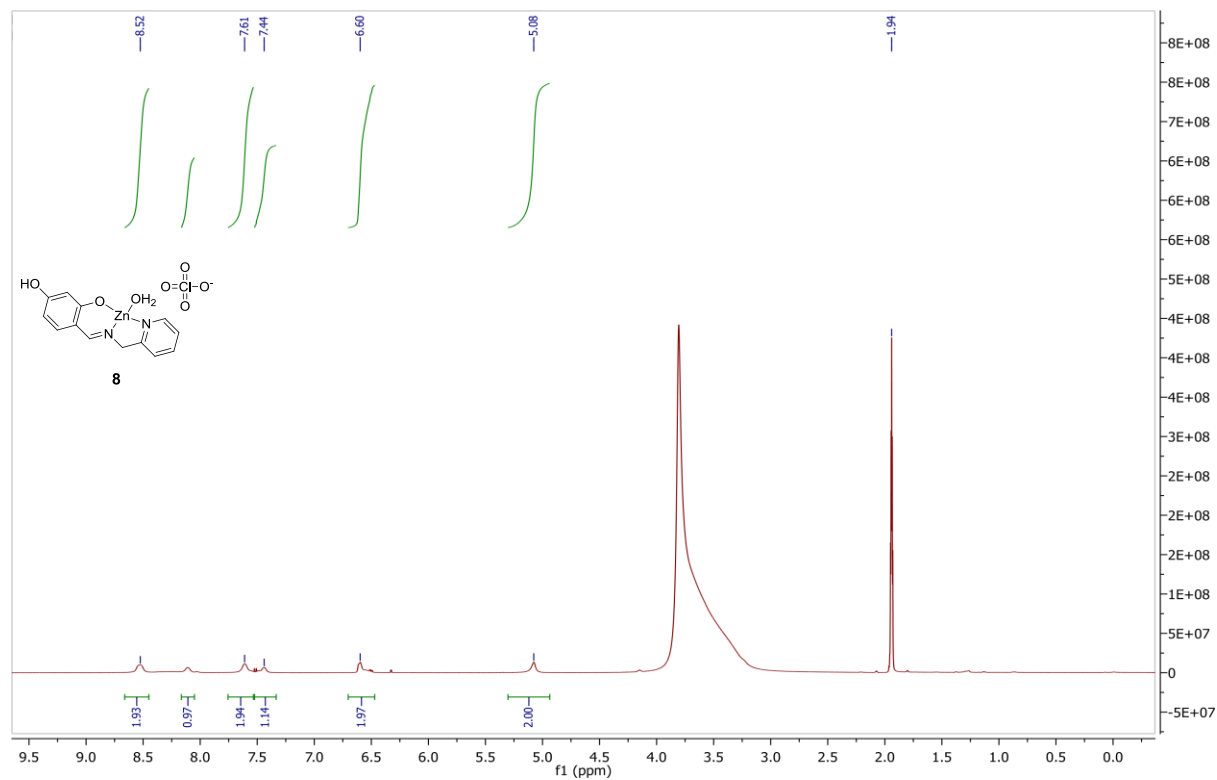
5.26 ¹³C NMR spectrum of 5-[2-(2,3,4,6-tetra-O-acetyl-β-D-glucopyranosyloxy)ethoxy)-2-
 {[2-methylpyridinyl)-E-imino]methyl}phenol **6d**



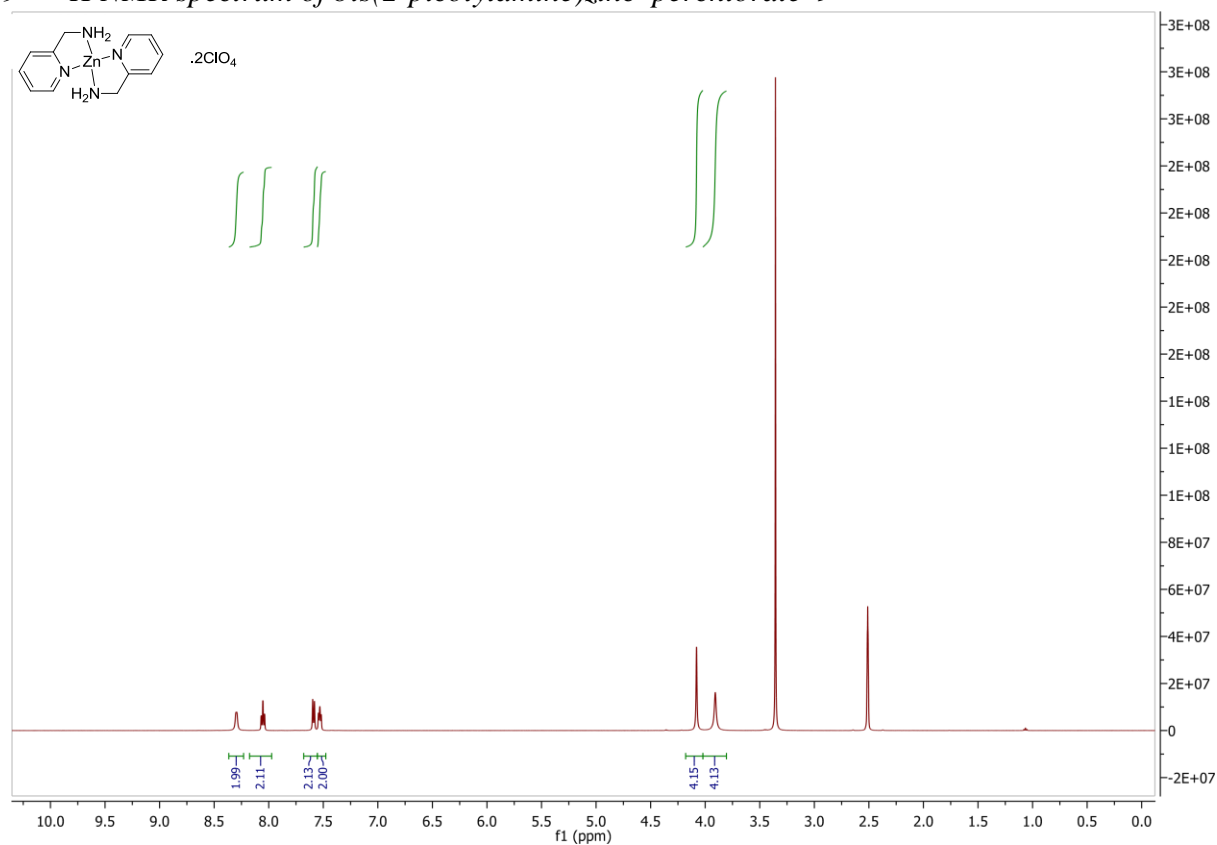
5.27 FTIR spectrum of aqua(5-hydroxy-2-[(2-methylpyridinyl)-E-imino]methyl}phenoate)copper perchlorate dihydrate **7**



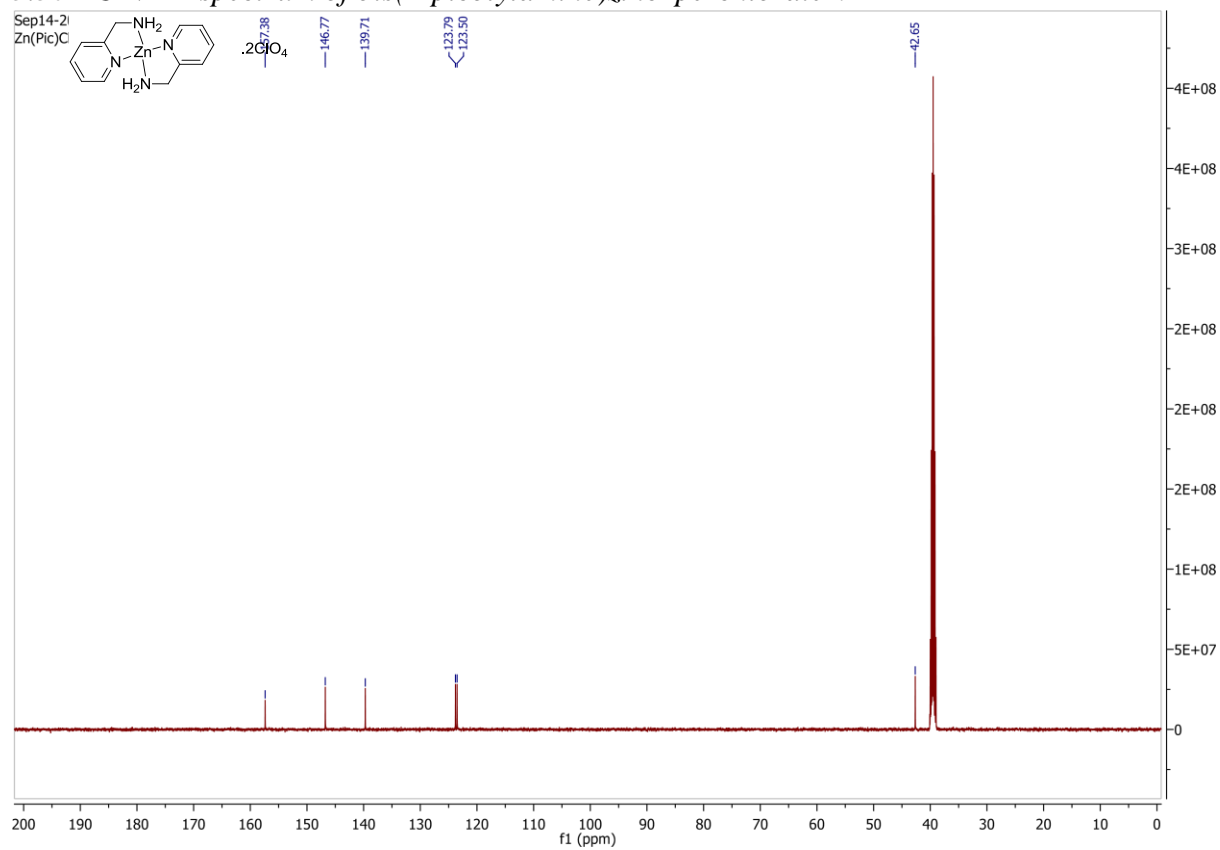
5.28 ^1H NMR spectrum of aqua(5-hydroxy-2-[(2-methylpyridinyl)-E-imino]methyl}phenoate)zinc perchlorate **8**



5.29 ^1H NMR spectrum of bis(2-picolylamine)zinc perchlorate **9**



5.30 ^{13}C NMR spectrum of bis(2-picolylamine)zinc perchlorate **9**



i Ferrari, E.; Lazzari, S.; Marverti, G.; Pignedoli, F.; Spagnolo, F.; Saladini, M. Synthesis, cytotoxic and combined cDDP activity of new stable curcumin derivatives. *Bioorg Med Chem* **2009**, *17*, 3043–3052.

ii Brunner, H.; Dafinger, W.; Schönenberger, H., Synthesis of PtCl₂ complexes of pyridylmethylamine ligands and their activity against hormone-dependent mammary carcinoma. *Inorganica Chimica Acta* **1989**, *156* (2), 291-301.

iii Mora-Soumille, N.; Al Bittar, S.; Rosa, M.; Dangles, O., Analogs of anthocyanins with a 3',4'-dihydroxy substitution: Synthesis and investigation of their acid-base, hydration, metal binding and hydrogen-donating properties in aqueous solution. *Dyes Pigments* **2013**, *96* (1), 7-15.

iv Hu, J. M.; Wang, X.; Qian, Y. F.; Yu, Y. Q.; Jiang, Y. Y.; Zhang, G. Y.; Liu, S. Y., Cytoplasmic Reactive Cationic Amphiphiles for Efficient Intracellular Delivery and Self-Reporting Smart Release. *Macromolecules* **2015**, *48* (16), 5959-5968.